Inorganic Chemistry

Article

pubs.acs.org/IC

1,2-Addition of Dihydrogen across Rhodium(III)−OMe Bonds

Samantha A. Burgess,[†] Deepa Devarajan,[‡] Tamara Bolaño,[†] Daniel H. Ess,*[,‡] T. Brent Gunnoe,*[,†] Michal Sabat,[§] and William H. Myers[∥]

[†]Department of Chemistry, University of Virginia, Charlottesville, Virginia 22904, United States

[‡]Department of Chemistry and Biochemistry, Brigham Young University, Provo, Utah 84602, United States

[§]Nanoscale Material Characterization Facility, Department of Materials Science and Engineering, University of Virginia, Charlottesville, Virginia 22904, United States

[∥]Department of Chemistry, University of Richmond, Richmond, Virginia 23173, United States

Supporting Information

ABSTRACT: The Rh(III) complexes $[(^t\text{bpy})_2\text{Rh(OMe)(L)}][X]_n$ (^{t}bpy = 4,4′-di-*tert*-butyl-2,2′-bipyridyl; L = MeOH, n = 2, X = OTf (OTf = trifluoromethanesulfonate), TFA (TFA = trifluoroacetate); L = TFA, n = 1, X = OTf) have been shown to activate dihydrogen via net 1,2-addition of the H−H bond across the Rh^{III}−OMe bond. The bis(methoxide) complex $[(^t\text{bpy})_2\text{Rh(OMe)}_2][\text{OTf}]$ was synthesized by addition of $CsOH{\cdot}H_2O$ in methanol to $[(^t\text{bpy})_2\text{Rh(OTf)}_2][\text{OTf}]$ in CH_3CN. The addition of HTFA to $[(^t\text{bpy})_2\text{Rh(OMe)}_2][\text{OTf}]$ leads to the formation of $[(^t\text{bpy})_2\text{Rh(OMe)(MeOH)}][\text{OTf}][\text{TFA}]$, which exists in equilibrium with $[(^t\text{bpy})_2\text{Rh(OMe)(TFA)}][\text{OTf}]$. The mixture of $[(^t\text{bpy})_2\text{Rh(OMe)(MeOH)}][\text{OTf}][\text{TFA}]$ and $[(^t\text{bpy})_2\text{Rh(OMe)(TFA)}][\text{OTf}]$ activates dihydrogen at 68 °C to give methanol and $[(^t\text{bpy})_2\text{Rh(H)(TFA)}][\text{OTf}]$. Studies indicate that the activation of dihydrogen has a first-order dependence on the Rh(III) methoxide complex and a dependence on hydrogen that is between zero and first order. Combined experimental and computational studies have led to a proposed mechanism for hydrogen activation by $[(^t\text{bpy})_2\text{Rh(OMe)(MeOH)}][\text{OTf}][\text{TFA}]$ that involves dissociation of MeOH, coordination of hydrogen, and 1,2-addition of hydrogen across the Rh−OMe bond. DFT calculations indicate that there is a substantial energy penalty for MeOH dissociation and a relatively flat energy surface for subsequent hydrogen coordination and activation.

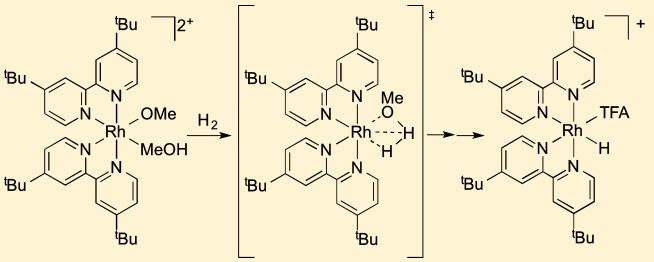

INTRODUCTION

The activation of covalent bonds (e.g., H−H, Si−H, and C−H bonds) is relevant to the development of catalytic reactions using dihydrogen, silanes, and hydrocarbons. For example, catalytic hydrogenations are among the most versatile and important synthetic processes.[1−3] For transition-metal-catalyzed hydrogenation reactions, the dihydrogen activation step usually occurs by oxidative addition to the metal to form a bis(hydride) complex or by 1,2-addition across a M−X (X = OR, NR_2, SR, etc.) bond to produce (H)M−X(H). The latter reaction is often considered heterolytic cleavage with formal transfer of a proton to the ligand X and transfer of a hydride to the metal (Scheme 1). Heterolytic cleavage of dihydrogen is likely involved in hydrogenations of aldehydes, ketones, and imines and in the generation of Stryker's reagent.[4,5]

Scheme 1. 1,2-Addition of Dihydrogen across M−X (X = OR, NR_2, SR) Bonds

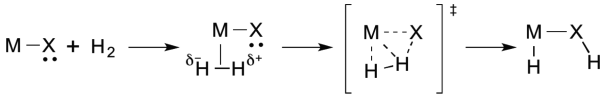

Furthermore, net dihydrogen addition across M−OR bonds could play a role in deoxygenation of biomass (or compounds that model biomass) via hydrogenolysis of ethers.[6,7]

Examples of stoichiometric dihydrogen or related C−H activations by d^6 hydroxide and amido complexes have been reported. For example, d^6 complexes have been demonstrated to activate dihydrogen and/or arene C−H bonds.[8,9] Complexes with d^8 configurations have also been shown to perform stoichiometric activation of H−H or C−H bonds. Goldberg and co-workers have reported dihydrogen activation by the d^8 Pd(II) complexes (PCP)Pd(OR) (PCP = 2,6-bis-$(CH_2P^tBu_2)_2C_6H_3$; R = H, CH_3)[10,11] and benzene C−H activation by d^8 Rh(I) complexes (PNP)Rh(X) (PNP = 2,6-((di-*tert*-butylphosphino)methyl)pyridine; X = OH, OCH_2CF_3).[12,13] Furthermore, the Ir(I) and Rh(I) complexes $[(\kappa^4\text{-COD})\text{M}(\mu\text{-OH})]_2$ (M = Rh, Ir; COD = 1,5-cyclooctadiene) activate C−H bonds of indene to give $[(\text{COD})\text{Rh}(\eta^3\text{-indenyl})]$.[14,15] Examples of both H−H activation and C−H activation across d^8 Pt^{II}−X bonds accelerated by Pt(0) particles are also known.[16,17] We reported that the net addition of H−H

Received: March 20, 2014
Published: May 7, 2014

   dx.doi.org/10.1021/ic500636m | *Inorg. Chem.* 2014, 53, 5328−5340

across the Pt−NHPh bond of [(^{t}bpy)Pt(Me)(NHPh)] is catalyzed by Pt(s).[16] Piers and co-workers reported benzene C−H addition across the Pt^{II}−OH bonds of (BIAN)Pt$(OH)_2$ (BIAN = bis(3,5-bis(2,6-diisopropylphenyl)benzene)-acenapthenequinonediimine), which is also accelerated by in situ generated Pt(0) particles.[17]

The half-sandwich complexes [Cp*M(PMe_3)(SDmp)]-[BAr′$_4$] (M = Rh, Ir; Dmp = 2,6-dimesitylphenyl; BAr′$_4$ = tetrakis[3,5-bis(trifluoromethyl)phenyl]borate) mediates heterolysis of dihydrogen to form [Cp*Rh(PMe_3)(H)(HSDmp)]-[BAr′$_4$], which hydrogenates benzaldehyde, *N*-benzylideneaniline, and cyclohexanone.[18] The heterolytic activation of dihydrogen by [Tp^{Me2}Rh$(SPh)_2$(NCMe)] (Tp^{Me2} = hydrotris-(3,5-dimethylpyrazolyl)borate) to form Tp^{Me2}Rh(H)(SPh)-(NCMe) and PhSH has been reported.[19,20]

We sought a robust Rh(III) complex supported by N-based ligands to study dihydrogen addition across Rh^{III}−OR bonds. Herein, we report the preparation of [(^{t}bpy)$_2$Rh$(OMe)_2$]$^+$ and its use as a precursor for heterolytic dihydrogen activation across a Rh^{III}−OMe bond.

RESULTS AND DISCUSSION

The reaction of [(^{t}bpy)$_2$Rh$(OTf)_2$][OTf] in CH_3CN with 2.5 equiv of CsOH·H_2O in MeOH at room temperature produces [(^{t}bpy)$_2$Rh$(OMe)_2$][OTf] (**1**) in 90% isolated yield (eq 1).

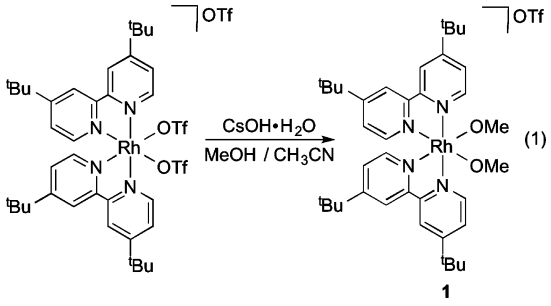

The ^{1}H NMR spectrum of **1** shows six ^{t}bpy aromatic resonances, two ^{t}Bu singlets, and one methoxide resonance (2.6 ppm), which is consistent with the expected C_2 symmetry. The Rh(III) complex [(^{t}bpy)$_2$Rh$(OMe)_2$]Cl was prepared using the same method as for complex **1** except [(^{t}bpy)Rh-$(Cl)_2$]Cl was used as the starting material. A metathesis reaction of [(^{t}bpy)$_2$Rh$(OMe)_2$]Cl with NaBAr′$_4$ leads to the formation of [(^{t}bpy)$_2$Rh$(OMe)_2$]BAr′$_4$ (**2**). A crystal of complex **2** suitable for an X-ray diffraction study was obtained (Figure 1). The structure of **2** confirms the expected pseudo-octahedral coordination sphere. The Rh−O1 and Rh−O2 bond lengths are 2.003(2) Å and 2.002(2) Å, respectively. The Rh−O1−C1 and Rh−O2−C2 bond angles are 117.8(2) Å and 117.2(2)°, respectively.

The addition of 1 equiv of HTFA (trifluoroacetic acid) to a suspension of complex **1** in THF results in a homogeneous solution (Scheme 2). After the solution is stirred for 12 h at room temperature, [(^{t}bpy)$_2$Rh$(MeOH)_2$][OTf][TFA]$_2$ (**3**) precipitates from solution as a yellow solid. ^{1}H NMR analysis of the filtrate after removing **3** by filtration indicates a mixture of the two (^{t}bpy)$_2$Rh complexes [(^{t}bpy)$_2$Rh(OMe)(MeOH)]-[OTf][TFA] (**4**) and [(^{t}bpy)$_2$Rh(OMe)(TFA)][OTf] (**5**) in an approximate 2:1 ratio. The ^{19}F NMR spectrum of the mixture of **4** and **5** contains a single OTf resonance at −80.1 ppm and two TFA resonances at −77.0 and −77.3 ppm.

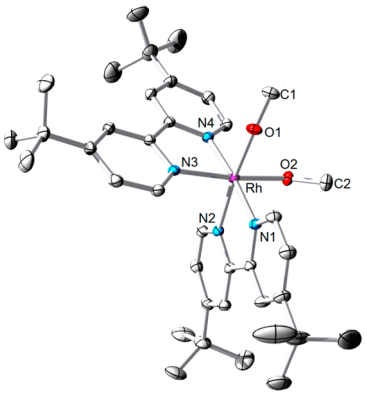

Figure 1. ORTEP diagram (50% probability ellipsoids) of [(^{t}bpy)$_2$Rh-$(OMe)_2$]BAr′$_4$ (**2**). Counterions and hydrogen atoms are omitted for clarity. Selected bond lengths (Å): Rh−N1, 2.048(2); Rh−N2, 2.017(2); Rh−N3, 2.049(2); Rh−N4, 2.022(2); Rh−O1, 2.003(2); Rh−O2, 2.002(2); O1−C1, 1.396(3); O2−C2, 1.402(3). Selected bond angles (deg): Rh−O1−C1, 117.8(2); Rh−O2−C2, 117.2(2); N4−Rh−N3, 96.84(9); O1−Rh−O2, 91.73(8); N1−Rh−N2, 79.68(9); N1−Rh−N4, 95.97(8); N2−Rh−N3, 96.84(9).

Scheme 2. Reaction of [(^{t}bpy)$_2$Rh$(OMe)_2$][OTf] (1) with HTFA (1 equiv) Leading to the Formation of Three Products

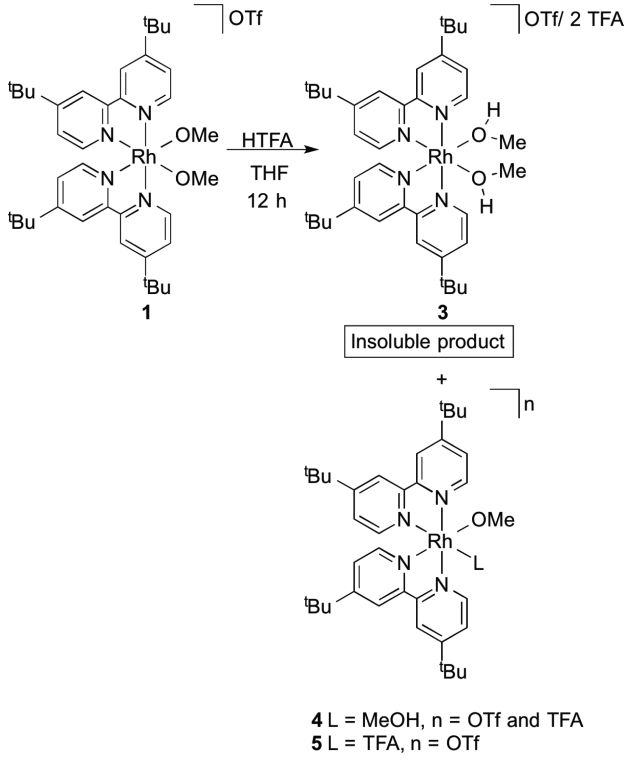

A crystal of complex **4** suitable for an X-ray diffraction study was obtained by layering a methylene chloride solution of complexes **3**−**5** with pentane (Figure 2). The Rh−O bond length of the methoxide ligand (Rh−O1 = 1.994(3) Å) is slightly shorter than that of the methanol ligand (Rh−O2 = 2.062(3) Å), and the O−C bond distance for the methoxide ligand (O1−C1 = 1.396(6) Å) is slightly shorter than the O−C bond distance for the methanol ligand (O2−C2 = 1.427(6) Å). The Rh−O−C bond angles for the methoxide and methanol ligands are 119.4(3)° and 121.0(3)°, respectively. When

dx.doi.org/10.1021/ic500636m | Inorg. Chem. 2014, 53, 5328−5340

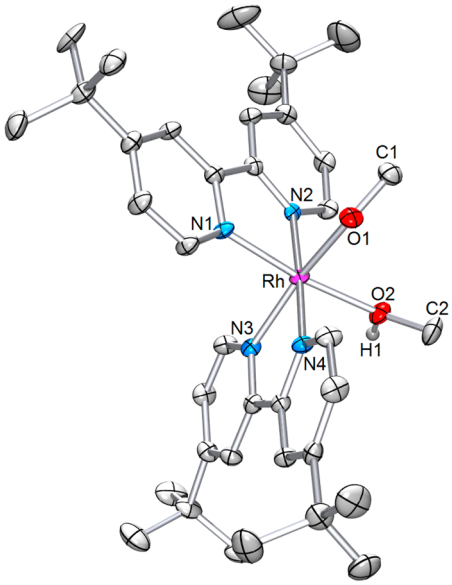

Figure 2. ORTEP diagram (50% probability ellipsoids) of [(^{t}bpy)$_2$Rh(OMe)(MeOH)][OTf][TFA] (**4**). Counterions and most hydrogen atoms are omitted for clarity. Selected bond lengths (Å): Rh−N1, 2.002(4); Rh−N2, 2.026(4); Rh−N3, 2.063(4); Rh−N4, 2.016(4); Rh−O1, 1.994(3); Rh−O2, 2.062(3); O1−C1, 1.396(6); O2−C2, 1.427(6). Selected bond angles (deg): Rh−O1−C1, 119.4(3); Rh−O2−C2, 121.0(3); N4−Rh−N3, 79.4(1); O1−Rh−O2, 89.4(1); N1−Rh−N2, 80.2(1); N1−Rh−N4, 97.4(1); N2−Rh−N3, 100.1(1).

crystals of **4** are dissolved in THF-d_8, the ^{1}H NMR spectrum shows a mixture of **4** and **5**. This result is consistent with the rapid establishment of an equilibrium between **4** and **5**.

The room-temperature ^{1}H NMR spectrum of [(^{t}bpy)$_2$Rh(OMe)(MeOH)][OTf][TFA] (**4**) contains a single resonance for the methoxide and methanol CH_3 groups, which is inconsistent with a static asymmetric complex. However, variable-temperature NMR spectroscopy revealed a dynamic process that is consistent with rapid proton exchange between the methanol and methoxide ligands. Density functional theory (DFT) calculations indicate a $\Delta H^{\ddagger}$ value of 3.1 kcal/mol and a $\Delta G^{\ddagger}$ value of 4.8 kcal/mol (298 K) for the intramolecular proton transfer (see the Supporting Information). Below room temperature, the sharp singlet at 2.83 ppm in the room-temperature ^{1}H NMR spectrum broadens (the coalescence temperature is observed at −36 °C) and partially resolves into two broad resonances at ∼3.0 and ∼2.7 ppm, which we assigned to the methoxide and methanol ligands. The slow exchange limit was not reached at −94 °C for the methanol and methoxide CH_3 protons. The response of the aromatic and ^{t}Bu resonances is also consistent with the proposed fluxional process. The coordinated MeOH ligand of **4** does not exchange with free MeOH on the NMR timescale. Thus, the fluxional process does not likely involve MeOH dissociation. Instead, we are observing an exchange of the OH proton between the MeOH and OMe ligands.

Heating (68 °C) a mixture of complexes **4** and **5** with dihydrogen (15−55 psig) produces free MeOH and [(^{t}bpy)$_2$Rh(H)(TFA)]$^+$ (**6**) (eq 2). Complex **5** is quickly consumed after pressurizing with dihydrogen and heating to 68 °C. The hydride complex [(^{t}bpy)$_2$Rh(H)(TFA)][OTf] (**6**) has been independently synthesized via the oxidative addition of HTFA to the Rh(I) complex [(^{t}bpy)$_2$Rh]$^+$ (eq 3). A Hg poisoning test was performed to test for possible formation of

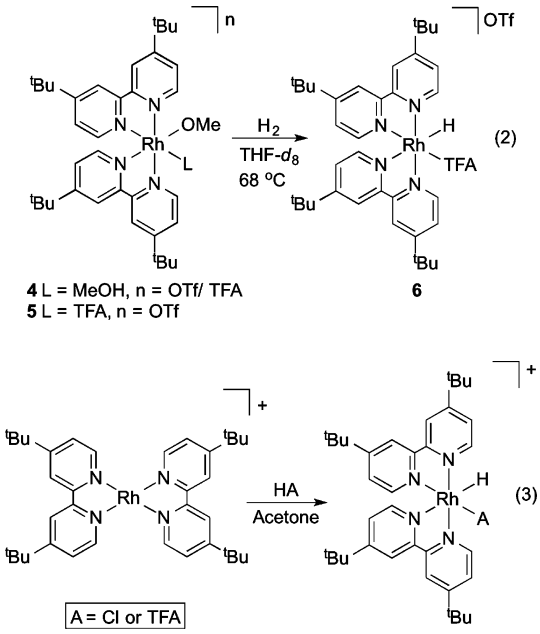

Rh nanoparticles,[21] but the rate of disappearance of complexes **4** and **5** was not significantly altered in the presence of Hg.

Under rigorous anaerobic conditions, complex **6** is stable in THF-d_8. However, in the absence of dihydrogen and without rigorous protection from air, complex **6** decomposes to [(^{t}bpy)$_3$Rh]$^{3+}$ and unknown products over a period of several hours at room temperature. In addition, the hydride complex **6** is sensitive to chloride sources. Failure to remove residual CH_2Cl_2 from the synthesis of [(^{t}bpy)$_2$Rh(OMe)$_2$][OTf] leads to the formation of the second hydride species [(^{t}bpy)$_2$Rh(H)(Cl)]$^+$ (−14.42 ppm, d, $^1J_{Rh-H}$ = 12 Hz) from the reaction of **6** and CH_2Cl_2. [(^{t}bpy)$_2$Rh(H)(Cl)][TFA] has been independently synthesized by the oxidative addition of HCl to [(^{t}bpy)$_2$Rh][TFA] (eq 3). When [(^{t}bpy)$_2$Rh(H)(TFA)][OTf] is dissolved in THF, CH_2Cl_2 (∼5 equiv) is added, the mixture is pressurized with dihydrogen (25 psig) and heated to 70 °C for 24 h, complete conversion to [(^{t}bpy)$_2$Rh(Cl)$_2$][TFA] (**8**) is observed (Scheme 3). In addition, the hydride complex **6** reacts (6.5 h, 70 °C) with excess CH_2Br_2 (19 equiv) to generate [(^{t}bpy)$_2$Rh(Br)$_2$][TFA] (**9**). The identity of **9** has been confirmed by independent synthesis (Scheme 4).

^{1}H NMR spectroscopy was used to monitor the reaction of **4** and **5** with hydrogen over a range of hydrogen pressures (15, 30, 45, and 55 psig). Unless otherwise noted, all kinetic experiments were performed at least in triplicate. Intermediates were not observed. Representative kinetic plots of concentration of Rh starting material versus time are shown in Figure 3. The range of initial hydrogen concentrations is 6.3×10^{-3} M (15 psig) to 1.8×10^{-2} M (55 psig), which gives an approximate 2.9-fold change in initial concentration from 15 to 55 psig. The dependence of rate on hydrogen concentration is not definitive. Two observations are consistent with a process that is zero order in dihydrogen and first order in Rh complex. First, good fits (R^2 = 0.96−0.99) for a first-order exponential decay fit are obtained as well as natural log plots (Table 1, Figures 3 and 4). Second, within deviations of the experiments, the rates of reaction show little dependence on concentration of dihydrogen between 15 and 45 psi (Figure 3 and Table 1). However, k_{obs} values (taken from first-order fits) indicate that the rate of reaction increases by a factor of ∼1.5 with a 2.9-fold

dx.doi.org/10.1021/ic500636m | Inorg. Chem. 2014, 53, 5328−5340

Scheme 3. Reaction of $[(^t\text{bpy})_2\text{Rh(H)(TFA)}][\text{OTf}]$ (6) with CH_2Cl_2 Leading to the Formation of a Second Hydride Species, $[(^t\text{bpy})_2\text{Rh(H)(Cl)}][\text{TFA}]$ (7), and Excess CH_2Cl_2 Leading to the Formation of $[(^t\text{bpy})_2\text{Rh(Cl)}_2][\text{TFA}]$ (8)[a]

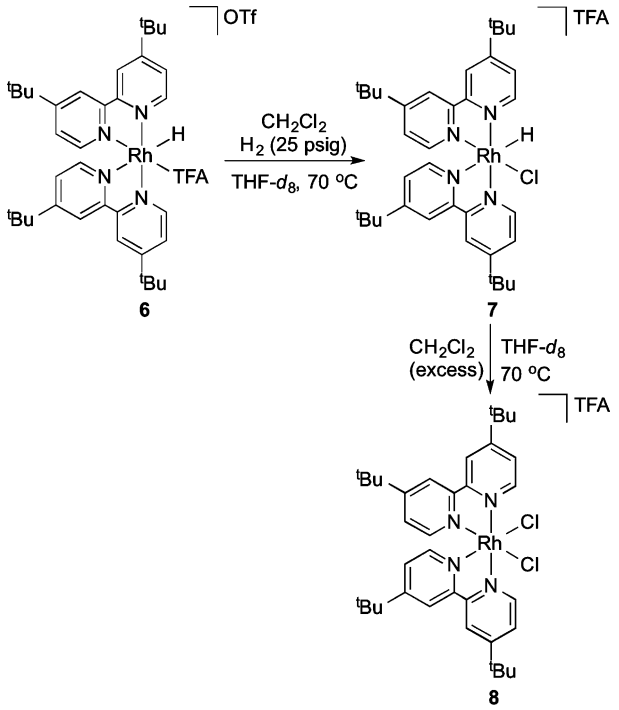

[a]The reaction is performed in the presence of H_2 to suppress decomposition of complex **6**.

Scheme 4. Reaction of $[(^t\text{bpy})_2\text{Rh(H)(TFA)}][\text{OTf}]$ (6) with Excess CH_2Br_2 Leading to the Formation of $[(^t\text{bpy})_2\text{Rh(Br)}_2][\text{TFA}]$ (9) without Observation of an Intermediate Hydride Species[a]

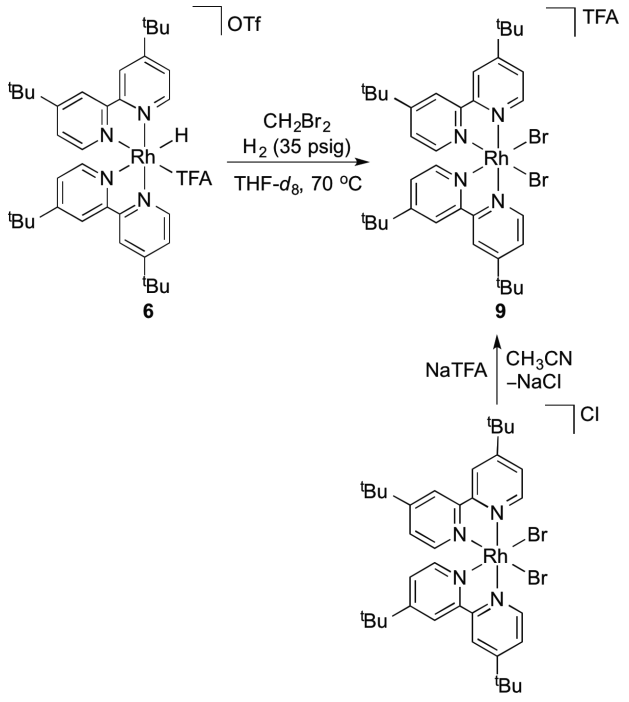

[a]The reaction is performed in the presence of H_2 to suppress decomposition of complex **6**.

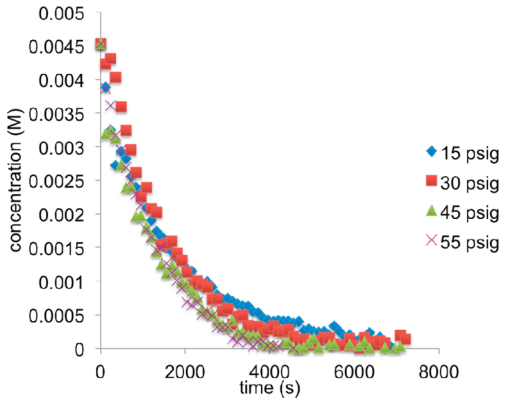

Figure 3. Disappearance of starting material (complexes **4** and **5**) under a variable pressure of dihydrogen.

Table 1. Average k_{obs} Values from the First-Order Fits to Kinetic Plots for the Reaction of 4 and 5 with H_2 at 68 °C[a]

H_2 (psig)	k_{obs} (10^{-4} s^{-1})[b]
15	5.4(7)
30	6.8(9)
45	5.1(9)
55	8.0(8)

[a]See Figure 3. [b]k_{obs} values are the average from at least three independent reactions.

increase in initial hydrogen concentration (comparing the results using 15 psig to those using 55 psig). Thus, the kinetic data point to a dependence on hydrogen concentration that is intermediate between zero and first order (see below).

We probed the influence of free methanol on the rate of dihydrogen activation (Table 2 and Figure 5). The reaction rate increases by a factor of approximately 2 from 0.002 M MeOH to 0.011 M of free MeOH. A plot of k_{obs} versus concentration of MeOH reveals a non-first-order acceleration (Figure 5). This is surprising, since MeOH dissociation likely precedes dihydrogen coordination to Rh (see below). This possibly suggests that two factors are at play for the influence of MeOH on the rate of hydrogen activation: (1) coordination chemistry with Rh and (2) adjustment of solvent polarity (see below). Efforts to perform the reaction in other polar solvents (e.g., CH_3NO_2, CH_3CN, acetone) resulted in decomposition of complexes **4** and **5** without production of **6**.

The rate of degenerate exchange between coordinated and free methanol was determined under pseudo-first-order conditions. In separate experiments, CD_3OD (5, 10, and 20 equiv relative to Rh) was added to a solution of complex **4** in THF-d_8. A plot of k_{obs} values (obtained from first-order fits for disappearance of the resonance for coordinated MeOH for **4**) versus the concentration of CD_3OD provides support that the reaction is zero order in MeOH (Figure 6). This is consistent with rate-limiting dissociation of MeOH (Scheme 5). The k values obtained for the fits of the first-order exponential decay plots (Table 3) are statistically identical or very similar to the k_{obs} values for the dihydrogen activation reaction (k_{obs} = [5.1(9)] × 10^{-4} s^{-1}) in the absence of added MeOH (0.002 M free MeOH; see Table 2). To test for a KIE for degenerate methanol exchange from $[(^t\text{bpy})_2\text{Rh}(CH_3OH)(OCH_3)]^{2+}$, we prepared $[(^t\text{bpy})_2\text{Rh}(CD_3OD)(OCD_3)]^{2+}$ and measured the rate of exchange between coordinated CD_3OD and free

dx.doi.org/10.1021/ic500636m | Inorg. Chem. 2014, 53, 5328−5340

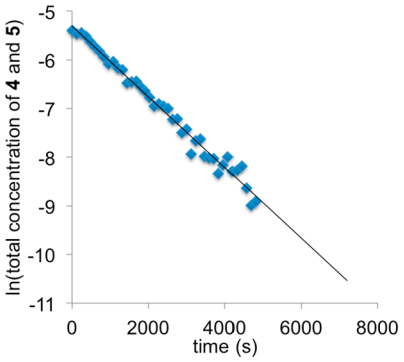

Figure 4. Representative plot of the natural log of total starting material (complexes **4** and **5**) versus time under 30 psig of dihydrogen (R^2 = 0.98).

Table 2. Average k_{obs} Values from the First-Order Decay Plots of the Reaction of Protonation Product with H_2 (45 psig) and Added MeOH (0, 3, and 5 equiv) at 68 °C

MeOH (equiv)	[MeOH] (M)	k_{obs} (s^{-1})[a]
0	0.002	[5.1(9)] × 10^{-4}
3	0.07	[7.1(9)] × 10^{-4}
5	0.11	[1.05(9)] × 10^{-3}

[a] k_{obs} values are the average from at least three independent reactions.

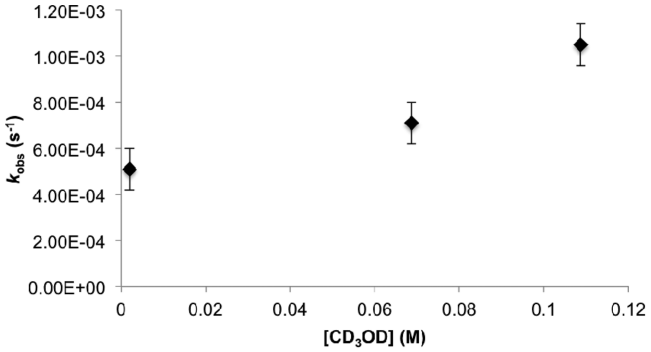

Figure 5. Plot of k_{obs} versus concentration of methanol for the activation of dihydrogen by complexes **4** and **5**.

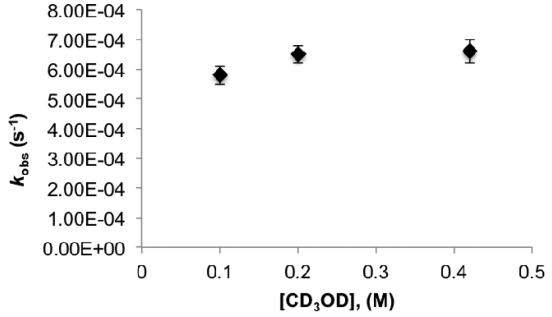

Figure 6. Plot of k_{obs} versus [CD_3OD] for the exchange of coordinated MeOH of [(^{t}bpy)$_2$Rh(OMe)(MeOH)][OTf][TFA] (**4**) with free CD_3OD.

CH_3OH. From three independent experiments [CH_3OH] = 0.1 M the first-order k_{obs} = [2.6(5)] × 10^{-4} s^{-1}. Thus, a KIE of k_H/k_D = 2.2(4) is observed for degenerate exchange of coordinated and free methanol using [(^{t}bpy)$_2$Rh(CH_3OH)(OCH_3)]$^{2+}$/CD_3OD (k_H) and [(^{t}bpy)$_2$Rh(CD_3OD)(OCD_3)]$^{2+}$/CH_3OH (k_D). Similarly, the half-life for H_2 activation by [(^{t}bpy)$_2$Rh(CD_3OD)(OCD_3)]$^{2+}$ is approximately 2.5 times greater than that using [(^{t}bpy)$_2$Rh(CH_3OH)(OCH_3)]$^{2+}$.

Scheme 5. Monitoring of the Rate of Coordinated MeOH Exchange with Free CD_3OD, Giving the Rate of MeOH Dissociation[a]

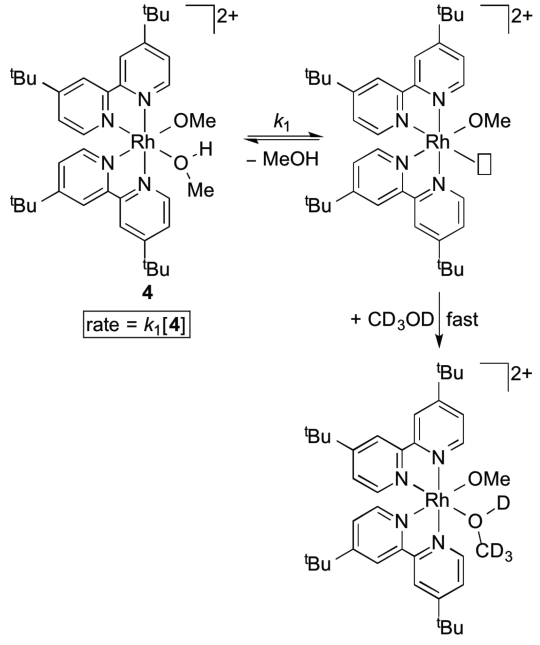

[a] See Table 3.

Table 3. Average k_{obs} Values from the First-Order Decay Plots for the Exchange of Coordinated MeOH of [(^{t}bpy)$_2$Rh(OMe)(MeOH)][OTf][TFA] (4) with CD_3OD at 68 °C

CD_3OD (equiv)	[CD_3OD] (M)	k_{obs} (10^{-4} s^{-1})[a]	$\Delta G^{\ddagger}$ (kcal/mol)
5	0.11	5.8(3)	25.0(2)
10	0.21	6.5(3)	25.0(1)
20	0.43	6.6(4)	25.1(1)

[a] k_{obs} values are the average from at least three independent reactions.

In order to determine whether or not a kinetic isotope effect (KIE) is observed when activating D_2, we reacted the mixture of **4** and **5** with D_2. The average k_{obs} from the first-order exponential decay plots for the reaction using 45 psig of D_2 (k_{obs} = [3.2(5)] × 10^{-4} s^{-1}) indicate that the reaction proceeds at a slightly faster rate with H_2 (k_{obs} = [5.1(9)] × 10^{-4} s^{-1}). Thus, the data are consistent with a small KIE with k_H/k_D = 1.6(4). No appreciable change in rate was observed upon varying the pressure of D_2 (we could not obtain the concentration of D_2 in the ^{1}H NMR experiments; k_{obs} = 5.1 × 10^{-4} s^{-1} (20 psig), 4.9 × 10^{-4} s^{-1} (30 psig), 4.9 × 10^{-4} s^{-1} (55 psig)). The high-pressure (>20 psig) experiments with D_2 were performed once.

When D_2 is used in place of H_2, the final deuteride product should be [(^{t}bpy)$_2$Rh(D)(TFA)][OTf] (Scheme 6). As expected, the hydride resonance at −13.3 ppm is initially absent in the ^{1}H NMR spectrum of the reactions using D_2. Eventually, the appearance of HD (4.50 ppm, $^1J_{HD}$ = 42 Hz) occurs simultaneously with the formation of the protio Rh−H complex [(^{t}bpy)$_2$Rh(H)(TFA)][OTf]. Additionally, free H_2 is observed. A source of H^+ (e.g., free MeOH) likely results in the

dx.doi.org/10.1021/ic500636m | Inorg. Chem. 2014, 53, 5328−5340

Scheme 6. Proposed Pathway for the Formation of HD, H_2, and Rh−H during the Reaction of $[(^tbpy)_2Rh(OMe)(MeOH)][OTf][TFA]$ (4) with D_2 after the Initial Formation of $[(^tbpy)_2Rh(D)(TFA)]^+$

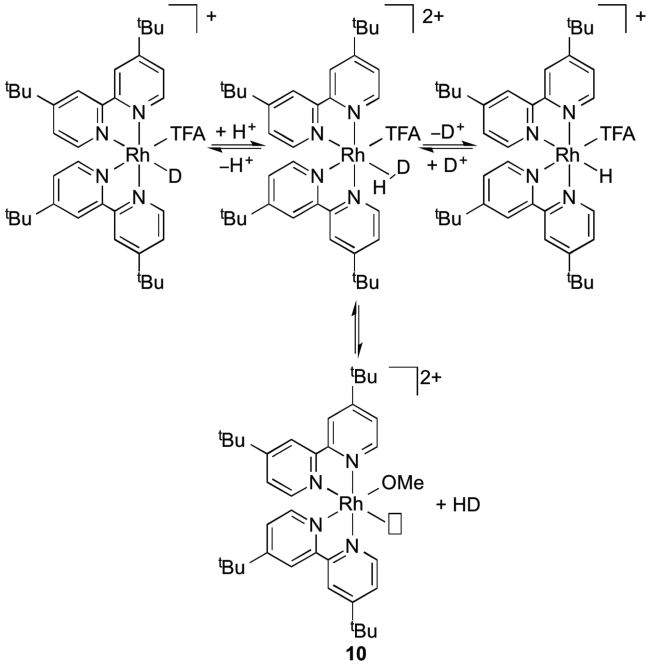

formation of Rh−H, HD, and H_2. As shown in Scheme 6, the initial product from the reaction with D_2, $[(^tbpy)_2Rh(D)(TFA)]^+$, can be protonated to form $[(^tbpy)_2Rh(\eta^2\text{-HD})(TFA)]^{2+}$, and the loss of D^+ would give $[(^tbpy)_2Rh(H)(TFA)]^+$. Exchange of D_2 with coordinated HD of $[(^tbpy)_2Rh(\eta^2\text{-HD})(TFA)]^{2+}$ would produce free HD.

Scheme 7 shows a likely pathway for the net 1,2-addition of H_2 across the Rh−OMe bond to form complex **6**. Methanol dissociation from $[(^tbpy)_2Rh(OMe)(MeOH)]^{2+}$ (**4**) would form the five-coordinate species $[(^tbpy)_2Rh(OMe)]^{2+}$ (**10**). Dihydrogen coordination gives $[(^tbpy)_2Rh(OMe)(\eta^2\text{-H}_2)][OTf][TFA]$, and 1,2-addition across the Rh−OMe bond produces the Rh−hydride product $[(^tbpy)_2R(H)(MeOH)]^{2+}$ (**11**). Complex **11** can convert to **6**, which is the final Rh product, by loss of MeOH and coordination of TFA.

In addition to experimental rate and isotope effects, we have also carried out density functional calculations to examine the structures and energy landscape for 1,2-addition of dihydrogen to complex **4**. All calculations were carried out with Gaussian 09.[22] Complex **4** was modeled without ^{t}Bu groups on the bpy ligands (**4′**). The M06[23,24] functional with the 6-31G(d,p)-[LANL2DZ for Rh] basis set and the pseudopotential were used to optimize all ground-state and transition-state structures. The larger basis set 6-311++G(2d,2p) (LANL2TZ(f) for Rh) was used for further refinement of energies. THF solvent effects were modeled with the implicit SMD model.[25]

To begin, we examined the energetics for MeOH loss to create a vacant coordination site on the Rh metal center in complex **4′** (Scheme 8, Figure 7). We did not examine associative mechanisms, since the Rh complex is an octahedral 18-electron species. As was somewhat expected, on the solvated potential energy surface no transition structure was located for direct MeOH dissociation. Therefore, the $\Delta H^{\ddagger}$ for MeOH dissociation and H_2 coordination is estimated by the thermodynamic enthalpy penalty for complete MeOH dissociation to give **10′**. The ΔH for MeOH dissociation is 22.2 kcal/mol relative to complex **4′**. We also examined the possibility that added MeOH can facilitate MeOH dissociation from the Rh coordination sphere. In accordance with Figure 6, the calculations suggest no acceleration of this process with added MeOH (see the Supporting Information for details).

After the five-coordinate complex **10′** is generated, dihydrogen can form a weak interaction with the Rh metal center to give the $[(bpy)_2Rh(OMe)(H_2)]^{2+}$ complex with ΔH = 15.4 kcal/mol (Scheme 8). Thus, coordination of hydrogen to **10′** is calculated to be exothermic by 6.8 kcal/mol. Similar to

Scheme 7. Proposed Mechanism for H_2 Activation by $[(^tbpy)_2Rh(OMe)(MeOH)[TFA][OTf]$ (4)

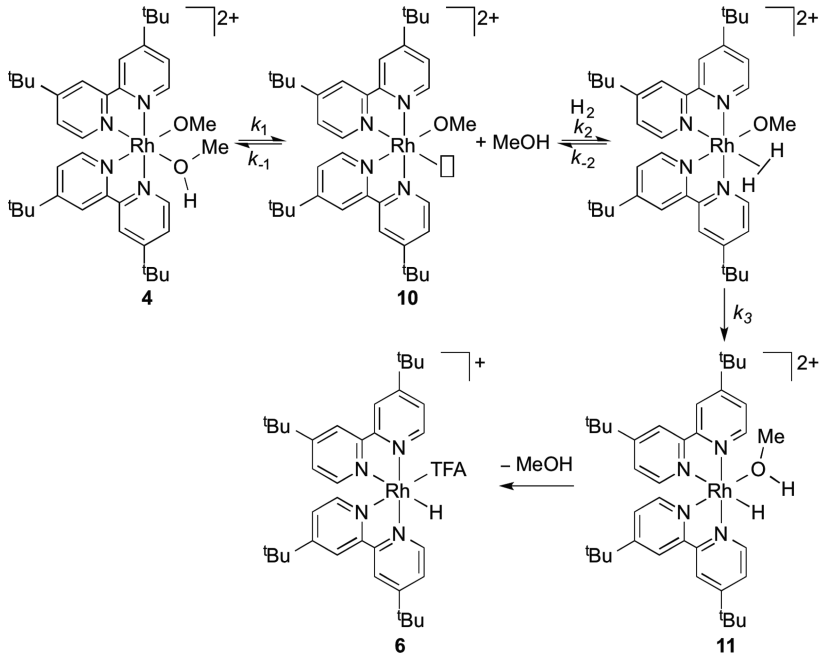

dx.doi.org/10.1021/ic500636m | Inorg. Chem. 2014, 53, 5328−5340

Scheme 8. Calculated Reaction Pathway for H_2 Activation by the Model Complex $[(bpy)_2Rh(OMe)(MeOH)]^{2+}$ (kcal/mol)

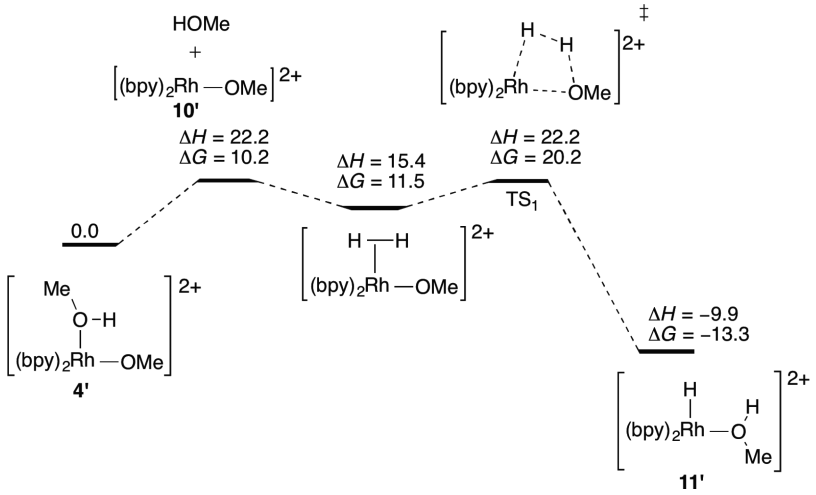

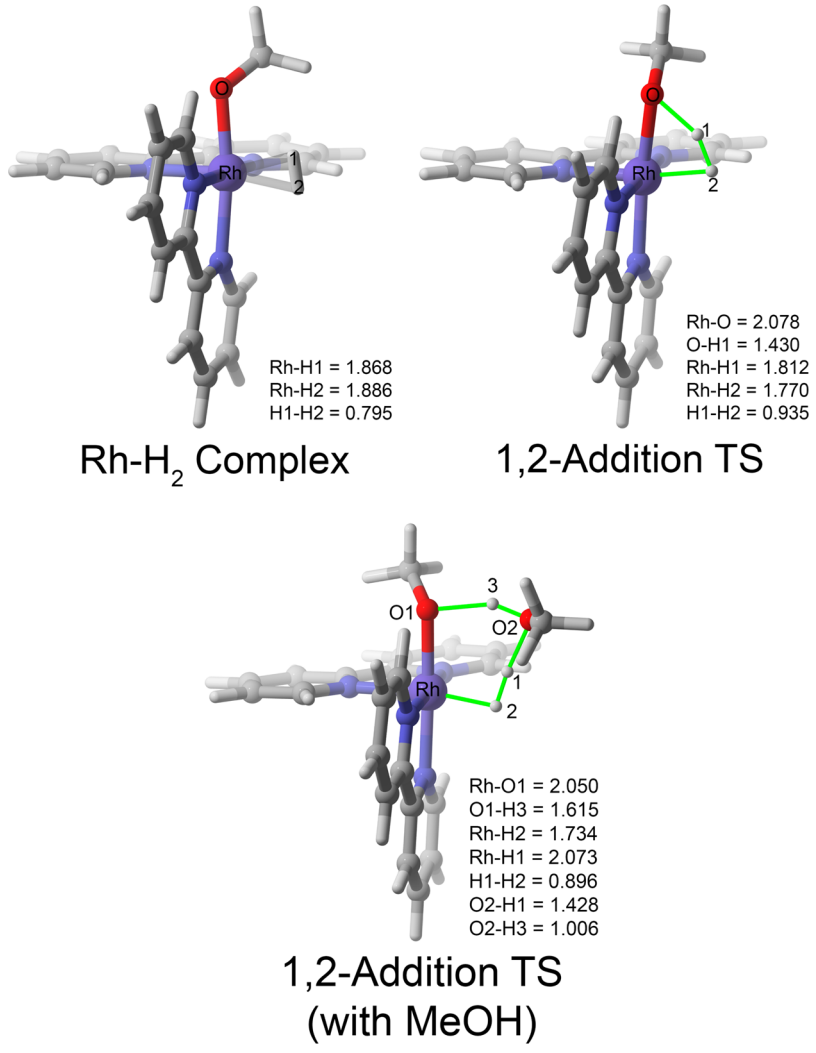

Figure 7. Dihydrogen coordination and 1,2-addition transition-state structures. Bond lengths are in Å.

the case for many other metal−H_2 coordination intermediates, the H−H bond length is stretched from its equilibrium bond length of 0.74 Å to 0.80 Å,[26,27] and the Rh−hydrogen interaction distances are between 1.87 and 1.89 Å.

After dihydrogen coordination there is a concerted transition state for 1,2-addition of H−H across the Rh−OMe bond that results in the Rh−H complex **11**′ (Scheme 8). In this transition state, the H−H is stretched to a partial bond length of 0.94 Å. The other geometrics, including the forming O−H bond and

dx.doi.org/10.1021/ic500636m | Inorg. Chem. 2014, 53, 5328−5340

forming Rh−H bond, are similar to previously reported 1,2-addition transition states to metal alkoxide species.[28,10,11,16,29,30] In the transition state there is also a short Rh−H interaction distance (1.81 Å) between the Rh metal center and the hydrogen that migrates from coordinated H_2 to the methoxide ligand.

The calculated $\Delta H^{\ddagger}$ value for 1,2-addition is 22.2 kcal/mol relative to complex **4′** and dihydrogen, and the resulting Rh−H species is −9.9 kcal/mol exothermic. While the Rh−H_2 coordination complex is stabilized by ∼7 kcal/mol relative to complex **10′**, overall the dihydrogen activation energy surface is flat for both coordination and cleavage of the H−H bond. On the basis of the enthalpy surface, dissociation of MeOH from complex **4′** is equal in energy to the dihydrogen activation transition state. This enthalpy landscape qualitatively matches the experimentally determined first-order rate dependence on Rh complexes and non-first-order rate dependence on dihydrogen pressure and could simultaneously explain the small KIE value observed if both transition states contribute to controlling the reaction rate. However, because a fully optimized transition state was not found for MeOH dissociation from complex **4′**, caution should be taken in the interpretation of a rate-limiting reaction step from this enthalpy surface.

While the calculated enthalpy landscape for dihydrogen coordination and 1,2-addition is in reasonable accordance with experiment, the free energy landscape is challenging to interpret. The ΔG value for MeOH dissociation and the energy of intermediate **10′** is 10.2 kcal/mol. However, this free energy value cannot be used to approximate the $\Delta G^{\ddagger}$ value for H_2 coordination, since MeOH is fully dissociated and the value highly overestimates translational entropy. In cases like this where the enthalpy surface is flat in the region for bond coordination and activation, caution should be used when interpreting the free energy landscape and it is likely best to examine the enthalpy landscape.

We have also examined the impact of added MeOH on the 1,2-addition transition state for dihydrogen activation. Figure 7 shows this transition state and how MeOH acts to shuttle the hydrogen during formation of the Rh−H species. Methanol has been previously shown to act as a proton shuttle in the isomerization of Ru hydrido alkynyl intermediates to Ru vinylidene complexes.[31] The $\Delta H^{\ddagger}$ and $\Delta G^{\ddagger}$ values for the MeOH-assisted pathway are 9.4 and 17.9 kcal/mol, respectively. This suggests that on the enthalpy surface there is a significant energetic advantage for MeOH to assist hydrogen transfer. However, this enthalpy advantage is significantly mitigated by an entropy penalty. On the free energy surface the MeOH-assisted transition state is ∼2 kcal/mol lower in energy than the transition state without MeOH. Corrections for the small concentration of added MeOH at 0.43 M shows that this MeOH assistance likely only accounts for an ∼1 kcal/mol lower activation free energy, which is possibly in accordance with the modest rate enhancement shown in Figure 5.

Rate law I in Scheme 9 is derived from the pathway in Scheme 7 using the steady-state approximation, and rate law II is the variant in which MeOH serves as a catalyst in the dihydrogen activation step (k_3). Both rate laws are consistent with the observed dependence on H_2 if the magnitude of $k_2k_3[H_2]$ is sufficiently large. That is, the $k_2k_3[H_2]$ term can cancel (or partially cancel) the first-order $[H_2]$ term in the numerator. The DFT calculations predict that the $\Delta H^{\ddagger}$ values for methanol dissociation and dihydrogen activation are similar

Scheme 9. Rate Laws Based on the Proposed Pathway Shown in Scheme 7 and a Variant with Methanol-Catalyzed H_2 Activation

$$\text{I. If } k_3 \text{ is RDS: Rate} = \frac{k_1k_2k_3[\text{Rh}][H_2]}{k_{-1}k_{-2}[\text{MeOH}] + k_{-1}k_3[\text{MeOH}] + k_2k_3[H_2]}$$

$$\text{II. Catalytic MeOH: Rate} = \frac{k_1k_2k_3[\text{Rh}][H_2][\text{MeOH}]}{k_{-1}k_{-2}[\text{MeOH}] + k_{-1}k_3[\text{MeOH}]^2 + k_2k_3[H_2][\text{MeOH}]}$$

(Scheme 8). Thus, it is not unreasonable that the $k_2k_3[H_2]$ term could compete with other terms in the denominators. The non-zero-order/non-first-order dependence on $[H_2]$ is also consistent with a small KIE for H_2 versus D_2 activation.

However, the rate laws (I and II) in Scheme 9 cannot account for the acceleration in rate as a function of increased [MeOH] even in the case of MeOH-catalyzed dihydrogen activation (rate law II). Both rate laws predict that increased [MeOH] would inhibit the rate of reaction. We propose that the MeOH acceleration is a result of a solvent polarity effect. As indicated above, we attempted to compare the rate of dihydrogen activation in THF with more polar solvents (CH_3NO_2, CH_3CN, acetone), but the reactions resulted in decomposition of complexes **4** and **5** without production of **6**. Another possibility is that the added MeOH aids dissociation of MeOH (k_1) via hydrogen bonding. To test this, we compared the impact of added CD_3OD on the activation of H_2 to that of CH_3OH. We cannot conclude whether or not there is an isotope effect for the MeOH acceleration for the reaction of **4** and **5** with dihydrogen in the presence of 3 equiv of MeOH versus 3 equiv of CD_3OD because the deviations are too large.

A small KIE is observed for activation of D_2 versus H_2. The activation of D_2 leads to the formation of CH_3OD (methanol-*d*), and we hypothesized that coordination of CH_3OD to Rh might affect the rate of methanol dissociation (k_1 in Scheme 5). Thus, if the reaction of **4** and **5** with D_2 leads to the formation of $[(^t\text{bpy})_2\text{Rh}(CH_3OD)(OCH_3)]^{2+}$, the k_H/k_D value observed for H_2/D_2 activation might be explained. However, our results suggest that $[(^t\text{bpy})_2\text{Rh}(CH_3OD)(OCH_3)]^{2+}$ likely does not form during D_2 activation by **4** and **5**. The activation of D_2 by **4** or **5** would produce $[(^t\text{bpy})_2\text{Rh}(CH_3OD)(H)]^{2+}$, which then dissociates CH_3OD to form **6**. Exchange of coordinated CH_3OH and free CH_3OD would likely require formation of the five-coordinate intermediate $[(^t\text{bpy})_2\text{Rh}(OCH_3)]^{2+}$, and our kinetic analysis suggests that this intermediate should react more rapidly with dihydrogen than with free methanol. However, it is possible to rationalize the small KIE for H_2 versus D_2 activation if the dependence on H_2 is intermediate between zero and first order. Thus, a relatively large KIE for H_2 versus D_2 would be attenuated by the non-first-order dependence. This scenario is consistent with a slight increase in rate of H_2 activation when the initial concentration is increased by a factor of 2.9 (see above). Unfortunately, the large deviations do not allow a quantified determination of the impact of H_2 concentration on rate.

SUMMARY

The addition of 1 equivalent of HTFA to $[(^t\text{bpy})_2\text{Rh}(OMe)_2][OTf]$ leads to the formation of $[(^t\text{bpy})_2\text{Rh}(OMe)(MeOH)][OTf][TFA]$ and $[(^t\text{bpy})_2\text{Rh}(OMe)(TFA)][OTf]$, which activate dihydrogen by net 1,2-addition of H−H across the Rh^{III}−OMe bond. The reaction displays non-first-order dependence on concentration of dihydrogen and a first-order

dx.doi.org/10.1021/ic500636m | Inorg. Chem. 2014, 53, 5328−5340

dependence on concentration of Rh starting material. The calculated $\Delta H^{\ddagger}$ for the H_2 activation step is only 6.8 kcal/mol from the dihydrogen adduct. In contrast, the calculated ΔH value for MeOH dissociation from $[(bpy)_2Rh(OMe)(MeOH)][TFA][OTf]$ (**4′**) is 22.2 kcal/mol. Thus, we propose that the dicationic charge of the $[(^tbpy)_2Rh(OMe)]^{2+}$ fragment affects the energetics of overall H_2 activation in two ways: (1) the enthalpy for dissociation of the Lewis basic methanol is relatively large and (2) the electrophilic character of the Rh(III) results in a very small $\Delta H^{\ddagger}$ value for the 1,2-addition of H_2 across the Rh−OMe bond. Thus, dihydrogen coordination to Rh(III) enhances its acidity,[32,26] and the basic methoxide can easily deprotonate the coordinated dihydrogen ligand. The addition of free MeOH provides a slight rate acceleration, and calculations predict that the participation of MeOH in the core unit for H_2 activation can lower the $\Delta H^{\ddagger}$ value. These results show promise for the use of highly electrophilic late transition metals with basic heteroatomic ligands (e.g., hydroxide, alkoxide, amido) for dihydrogen activation chemistry and the use of basic additives as cocatalysts.

EXPERIMENTAL SECTION

General Considerations. Unless otherwise noted, all synthetic procedures were performed under anaerobic conditions in a nitrogen-filled glovebox or by using standard Schlenk techniques. Glovebox purity was maintained by periodic nitrogen purges and was monitored by an oxygen analyzer (O_2(g) <15 ppm for all reactions). Toluene, tetrahydrofuran, and diethyl ether were dried by distillation from sodium/benzophenone. Pentane was distilled over P_2O_5. Acetonitrile and methanol were dried by distillation from CaH_2. Hexanes, benzene, and dichloromethane were purified by passage through a column of activated alumina. Acetonitrile-d_3, methylene chloride-d_2, acetone-d_6, and THF-d_8 were stored under a N_2 atmosphere over 4 Å molecular sieves. H_2 and D_2 were purchased from Matheson Gas and Cambridge Isotope Laboratories, respectively, and used as received. ^{1}H and ^{13}C NMR spectra were recorded on a Varian Mercury Plus 300 MHz spectrometer (75 MHz operating frequency for ^{13}C NMR), Varian Inova 500 MHz spectrometer (125 MHz operating frequency for ^{13}C NMR), Bruker Avance DRX 600 MHz spectrometer (150 MHz operative frequency for ^{13}C NMR), or Bruker Avance III 800 MHz spectrometer (201 MHz operative frequency for ^{13}C NMR). All ^{1}H and ^{13}C NMR spectra are referenced against residual proton signals (^{1}H NMR) or the ^{13}C resonances of the deuterated solvent (^{13}C NMR). ^{19}F NMR (operating frequency 282 MHz) spectra were obtained on a Varian Mercury Plus 300 MHz spectrometer and referenced against an external standard of hexafluorobenzene (δ −164.9). Elemental analyses were performed by Atlantic Microlabs, Inc. High-resolution mass spectra were acquired in ESI mode from samples dissolved in a 3/1 acetonitrile/water solution containing sodium trifluoroacetate (NaTFA). Mass spectra are reported as M^+ for monocationic complexes or as $[M + H^+]$ or $[M + Na^+]$ for neutral complexes, using $[Na(NaTFA)_x]^+$ clusters as an internal standard. In all cases, observed isotopic envelopes were consistent with the molecular composition reported. For products with a simple spectrum, the monoisotopic ion is reported; for products with a complicated spectrum, the major peaks in the isotopic envelope are reported. Spectra were collected on either a Shimadzu IT-TOF or an Agilent 6230 TOF instrument. The preparation of $NaBAr'_4$ has been previously reported.[33] The ^{t}bpy versions of $[(bpy)_2Rh(X)_2]X$ (X = Cl, Br) were synthesized following the published procedure.[34] $(COE)_2Rh(TFA)$ (COE = cyclooctene) was made following the literature procedure using AgTFA instead of $AgPF_6$.[35] The synthesis of $[(bpy)_2Rh(H)(OTf)]^+$ has been previously reported without full experimental details or characterization data.[36] The oxidative additions of HTFA and HCl to $[(^tbpy)_2Rh]^+$, to form $[(^tbpy)_2Rh(H)(TFA)]^+$ and $[(^tbpy)_2Rh(H)(Cl)]^+$, respectively, were based on this synthesis.

$[(^tbpy)_2Rh(OTf)_2][OTf]$. This complex was prepared with modification to the procedure reported by Meyer and co-workers.[34] The complex $[(^tbpy)_2RhCl_2]Cl$ (0.4995 g, 0.6695 mmol) was dissolved in 1,2-dichlorobenzene (24 mL). HOTf (355 μL, 4.01 mmol) was added via a microsyringe. The yellow solution was heated at reflux overnight. When the mixture was cooled to room temperature, Et_2O (20 mL) was added through the condenser. The reaction mixture was placed in the freezer for several hours to allow maximum precipitation. The solid was collected by filtration through a fine-porosity frit, washed with Et_2O, and dried under vacuum for approximately 1 h. In air, the solid was reconstituted in CH_2Cl_2 and washed with H_2O (3 × 100 mL). The combined organic extracts were washed with brine (1 × 100 mL), dried over Na_2SO_4, and reduced to dryness using a rotary evaporator. The yellow solid was dried under vacuum overnight. The solid was reconstituted in CH_2Cl_2 and reprecipitated with Et_2O. The solid was collected over a fine-porosity frit, washed with Et_2O, and dried under vacuum (0.522 g, 72%). ^{1}H NMR (300 MHz, CD_3CN): δ 9.19 (d, $^3J_{H5-H6}$ = 6 Hz, 2H, ^{t}bpy 6/6′), 8.65 (d, $^4J_{H3-H5}$ = 2 Hz, 2H, ^{t}bpy 3/3′), 8.47 (d, $^4J_{H3-H5}$ = 2 Hz, 2H, ^{t}bpy 3/3′), 8.21 (dd, $^3J_{H5-H6}$ = 6 Hz, $^4J_{H3-H5}$ = 2 Hz, 2H, ^{t}bpy 5/5′), 7.45 (dd, $^3J_{H5-H6}$ = 6 Hz, $^4J_{H3-H5}$ = 2 Hz, 2H, ^{t}bpy 5/5′), 7.36 (d, $^3J_{H5-H6}$ = 7 Hz, 2H, ^{t}bpy 6/6′), 1.58, 1.37 (each a s, 18H, ^{t}Bu). ^{13}C NMR (75 MHz, CD_3CN): δ 169.7, 169.1, 158.6, 156.5, 152.9, 150.9, 127.8, 127.2, 124.4, 124.2 (each a s, ^{t}bpy aromatic C's), 37.3, 36.9 (each a s, ^{t}Bu $C(CH_3)_3$) 30.5, 30.2 (each a s, ^{t}Bu $C(CH_3)_3$). A quartet for O_3SCF_3 was not observed in the ^{13}C NMR spectrum. ^{19}F NMR (282 MHz, CD_3CN): δ −79.7 (s, OTf). Anal. Calcd for $C_{39}H_{48}F_9N_4O_9RhS_3$: C, 43.10; H, 4.45; N, 5.15. Found: C, 42.61; H, 4.25; N, 5.04.

$[(^tbpy)_2Rh(OMe)_2][OTf]$ (1). A solution of $[(^tbpy)_2Rh(OTf)_2][OTf]$ (0.1999 g, 0.1839 mmol) in CH_3CN (~10 mL) was slowly added to a solution of $CsOH·H_2O$ (0.0775 g, 0.462 mmol) in methanol (~5 mL). The yellow solution was stirred at room temperature for 1 h before the solvent was removed under vacuum. The yellow solid was dissolved in CH_2Cl_2 and the solution filtered through a plug of Celite. The Celite was washed with CH_2Cl_2 (5 × 5 mL). The filtrate was reduced to ~2 mL under vacuum. Pentane (5 mL) was added to precipitate a yellow solid. The solid was collected over a fine-porosity frit and then dried under vacuum before being transferred to a pressure tube. Pentane (~20 mL) was added, and the heterogeneous solution was stirred at room temperature overnight. The pressure tube was sonicated for 1 h. The solid was collected over a fine-porosity frit, washed with additional pentane (2 × 5 mL), and dried under vacuum (0.142 g, 90%). ^{1}H NMR (300 MHz, CD_3CN): δ 9.37 and 7.42 (each a d, $^3J_{H5-H6}$ = 6 Hz, 2H each, ^{t}bpy 6/6′), 8.51, 8.41 (each a d, $^4J_{H3-H5}$ = 2 Hz, 2H each, ^{t}bpy 3/3′), 7.9, 7.35 (dd, $^3J_{H5-H6}$ = 6 Hz, $^4J_{H3-H5}$ = 2 Hz, 2H each, ^{t}bpy 5/5′), 2.62 (bs, 6H, OCH_3), 1.55, 1.36 (each a s, 18H each, ^{t}Bu). ^{13}C NMR (75 MHz, CD_2Cl_2): δ 165.9, 164.6, 156.6, 155.7, 150.2, 149.7, 125.5, 124.9, 120.9, 120.7 (each a s, ^{t}bpy aromatic C's), 56.7 (s, OCH_3), 36.4, 36.1 (each a s, $C(CH_3)_3$), 30.8, 30.5 (each a s, $C(CH_3)_3$). ^{19}F NMR (282 MHz, CD_2Cl_2): δ −79.1 (s, OTf). Anal. Calcd for $C_{39}H_{54}F_3N_4O_5Rh$: C, 55.05; H, 6.40; N, 6.58. Found: C, 55.22; H, 6.40; N, 6.49.

$[(^tbpy)_2Rh(OMe)_2]Cl$. A procedure analogous to the synthesis of $[(^tbpy)_2Rh(OMe)_2][OTf]$ was employed, except $[(^tbpy)_2Rh(Cl)_2]Cl$ (0.2529 g, 0.3390 mmol) was used as the starting material (0.2288 g, 92%). ^{1}H NMR (300 MHz, CD_3CN): δ 9.38 (d, $^3J_{H5-H6}$ = 6 Hz, 2H, ^{t}bpy 6/6′), 8.53 (d, $^4J_{H3-H5}$ = 2 Hz, 2H, ^{t}bpy 3/3′), 8.43 (d, $^4J_{H3-H5}$ = 2 Hz, 2H, ^{t}bpy 3/3′), 7.97 (dd, $^3J_{H5-H6}$ = 6 Hz, $^4J_{H3-H5}$ = 2 Hz, 2H, ^{t}bpy 5/5′), 7.42 (d, $^3J_{H5-H6}$ = 6 Hz, 2H, ^{t}bpy 6/6′), 7.33 (dd, $^3J_{H5-H6}$ = 6 Hz, $^4J_{H3-H5}$ = 2 Hz, 2H, ^{t}bpy 5/5′), 2.63 (s, 6H, OCH_3), 1.55, 1.36 (each a s, 18H each, ^{t}Bu). ^{13}C NMR (151 MHz, CD_2Cl_2): δ 166.18, 164.95, 156.74, 155.99, 149.91, 149.67, 125.18, 124.71, 121.93, 121.78 (each a s, ^{t}bpy aromatic C's), 56.0 (OCH_3), 36.6, 36.3 (each a s, $C(CH_3)_3$), 30.9, 30.6 (each a s, $C(CH_3)_3$). MS (M^+ = $C_{38}H_{54}N_4O_2Rh^+$; m/z obsd, m/z calcd, ppm): 701.3308, 701.3296, 1.7.

$[(^tbpy)_2Rh(OMe)_2][BAr'_4]$ (2). $[(^tbpy)_2Rh(OMe)_2]Cl$ (0.1877 g, 0.2546 mmol) was partially dissolved in THF (~20 mL). $NaBAr'_4$ (0.2256 g, 0.2546 mmol) in THF (~5 mL) was added dropwise. The resulting solution was stirred at room temperature for 1 h before

dx.doi.org/10.1021/ic500636m | Inorg. Chem. 2014, 53, 5328−5340

reducing the solvent volume to 10 mL under vacuum. The solution was filtered through Celite to remove NaCl. The Celite was washed with THF (5 × 10 mL). The filtrate was reduced to dryness in vacuo. The resulting yellow solid was taken up in Et_2O and transferred to a vial. The Et_2O was removed under vacuum to yield an orange-yellow low-density solid. The solid was dried further under vacuum (0.3789 g, 95%). X-ray-quality crystals were grown by layering a solution of complex **2** in Et_2O with hexane. ^{1}H NMR (300 MHz, CD_3CN): δ 9.38 (d, $^3J_{H5-H6}$ = 6 Hz, 2H, ^{t}bpy 6/6′), 8.51 (s, 2H, ^{t}bpy 3/3′), 8.41 (s, 2H, ^{t}bpy 3/3′), 7.97 (dd, $^3J_{H5-H6}$ = 6 Hz, $^4J_{H3-H5}$ = 2 Hz, 2H, ^{t}bpy 5/5′), 7.73−7.63 (m, 12H, BAr′$_4$), 7.42 (d, $^3J_{H5-H6}$ = 6 Hz, 2H, ^{t}bpy 6/6′), 7.33 (dd, $^3J_{H5-H6}$ = 6 Hz, $^4J_{H3-H5}$ = 2 Hz, 2H, ^{t}bpy 5/5′), 2.63 (s, 6H, OCH_3), 1.55, 1.35 (each a s, 18H, ^{t}Bu). ^{13}C NMR (201 MHz, CD_3CN): δ 166.3, 165.2, 125.3, 125.3, 122.2, 122.2, 157.1, 156.5, 150.8, 149.8 (each a s, ^{t}bpy aromatic C's), 162.6 (q, $^1J_{B-Cipso}$ = 50 Hz, BAr′$_4$), 135.6 (BAr′$_4$), 129.9 (q, $^2J_{C-F}$ = 32 Hz, 31 Hz, *m*-BAr′$_4$), 125.4 (q, $^1J_{C-F}$ = 272 Hz, CF_3−BAr′$_4$), 118.7 (BAr′$_4$), 55.9 (s, OCH_3), 36.7, 36.4 (each a s, $C(CH_3)_3$), 30.6, 30.3 (each a s, $C(CH_3)_3$). ^{19}F NMR (282 MHz, CD_3CN): δ −63.6 (s, BAr′$_4$). MS ($M^+ = C_{38}H_{54}N_4O_2Rh^+$; *m*/*z* obsd, *m*/*z* calcd, ppm): 701.3304, 701.3296, 1.1.

[(^{t}bpy)$_2$Rh(OMe)$_2$][TFA]. [(^{t}bpy)$_2$Rh(OMe)$_2$]Cl (0.2288 g, 0.3104 mmol) was suspended in CH_3CN (∼25 mL). NaTFA (0.0425 g, 0.312 mmol) in CH_3CN (∼5 mL) was added dropwise. [(^{t}bpy)$_2$Rh(OMe)$_2$]Cl dissolved completely upon addition of NaTFA, and the solution became slightly cloudy. The resulting mixture was stirred at room temperature for 1 h before it was evaporated to dryness in vacuo. The yellow residue was dissolved in CH_2Cl_2 and filtered through Celite. The Celite was washed with CH_2Cl_2 (5 × 5 mL). The filtrate was reduced to dryness under vacuum. The yellow solid was reconstituted in CH_2Cl_2 and precipitated with pentane. The solid was combined with pentane (∼15 mL) and sonicated for 1 h. The solid was collected by filtration through a fine-porosity frit, washed with additional pentane, and dried under vacuum (0.2200 g, 87%). ^{1}H NMR (800 MHz, CD_3CN): δ 9.38 (d, $^3J_{H5-H6}$ = 6 Hz, 2H, ^{t}bpy 6/6′), 8.53 (d, $^4J_{H3-H5}$ = 2 Hz, 2H, ^{t}bpy 3/3′), 8.43 (d, $^4J_{H3-H5}$ = 2 Hz, 2H, ^{t}bpy 3/3′), 7.97 (dd, $^3J_{H5-H6}$ = 6 Hz, $^4J_{H3-H5}$ = 2 Hz, 2H, ^{t}bpy 5/5′), 7.42 (d, $^3J_{H5-H6}$ = 6 Hz, 2H, ^{t}bpy 6/6′), 7.34 (dd, $^3J_{H5-H6}$ = 6 Hz, $^4J_{H3-H5}$ = 2 Hz, 2H, ^{t}bpy 5/5′), 2.62 (s, 3H, OCH_3), 1.55, 1.36 (each a s, 18H, ^{t}Bu). ^{13}C NMR (201 MHz, CD_3CN): δ 166.3, 165.2, 157.1, 156.5, 150.8, 149.9, 125.4, 125.3, 122.3, 122.2 (each a s, ^{t}bpy aromatic C's), 55.9 (s, OCH_3), 36.7, 36.4 (each a s, $C(CH_3)_3$), 30.7, 30.3 (each a s, 3C, $C(CH_3)_3$). ^{19}F NMR (282 MHz, CD_3CN): δ −75.5 (s, TFA).

[(^{t}bpy)$_2$Rh(H)(TFA)][OTf] (6). *Method 1.* Exclusion of chlorinated solvents is critical for the synthesis of complex **6**. THF was freshly distilled prior to use. [(^{t}bpy)$_2$Rh(OMe)$_2$][OTf] (0.0606 g, 0.0712 mmol) was suspended in THF (∼15 mL) in a glass Fisher-Porter reactor. HTFA (5.5 μL, 0.072 mmol) was added via a microsyringe. Upon addition of acid, [(^{t}bpy)$_2$Rh(OMe)$_2$][OTf] dissolved and the solution changed from a bright yellow to a lighter yellow. The vessel was pressurized with 30 psig of H_2 and heated at 70 °C in an oil bath for 17 h. After heating, the solution was a dark purple. After the solution was cooled to room temperature, the solvent was decanted from any insoluble species and then removed in vacuo to yield a dark purple solid that was dried further under vacuum (0.059 g, 91%).

Method 2. [(^{t}bpy)$_2$Rh][TFA] (0.0050 g, 0.0066 mmol) was dissolved in acetone-d_6 in a screw-cap NMR tube. HTFA (10.2 μL of solution, 0.00663 mmol, 0.65 M in acetone-d_6) was slowly added via a microsryinge. The purple solution turned brown and then black. The product was analyzed by ^{1}H NMR spectroscopy but was not isolated. The ^{1}H NMR (300 MHz, THF-d_8): δ 9.43 (d, $^3J_{H5-H6}$ = 6 Hz, 1H, ^{t}bpy 6), 8.80 (d, $^3J_{H5-H6}$ = 6 Hz, 1H, ^{t}bpy 6), 8.66 (d, $^4J_{H3-H5}$ = 2 Hz, 1H, ^{t}bpy 3), 8.58 (d, $^4J_{H3-H5}$ = 2 Hz, 1H, ^{t}bpy 3), 8.52 (d, $^3J_{H5-H6}$ = 6 Hz, 2H, ^{t}bpy 6), 7.99 (dd, $^3J_{H5-H6}$ = 5 Hz, $^4J_{H3-H5}$ = 2 Hz, 1H, ^{t}bpy 5), 7.95 (dd, $^3J_{H5-H6}$ = 6 Hz, $^4J_{H3-H5}$ = 2 Hz, 1H, ^{t}bpy 5), 7.74 (dd, $^3J_{H5-H6}$ = 6 Hz, $^4J_{H3-H5}$ = 2 Hz, 1H, ^{t}bpy 5), 7.55 (dd, $^3J_{H5-H6}$ = 6 Hz, $^4J_{H3-H5}$ = 2 Hz, 1H, ^{t}bpy 5), 7.52 (d, $^4J_{H3-H5}$ = 1 Hz, 2H, ^{t}bpy 3), 1.53 (s, 9H, ^{t}Bu), 1.52 (s, 9H, ^{t}Bu), 1.38 (s, 9H, ^{t}Bu), 1.33 (s, 9H, ^{t}Bu), −13.36 (d, $^1J_{Rh-H}$ = 13 Hz, 1H, Rh−H). ^{13}C NMR (201 MHz, THF-d_8): δ 162.8, 162.2, 161.9, 161.7, 156.2, 154.8, 154.4, 154.3, 152.2, 148.8, 146.4, 146.2, 123.3, 122.5, 122.5, 122.4, 119.6, 119.6, 118.7 (each a s, ^{t}bpy aromatic C's, one signal missing presumably due to coincidental overlap), 33.9, 33.6, 33.5, 33.4 (each a s, $C(CH_3)_3$), 27.7, 27.7, 27.6, 27.5 (each a s, $C(CH_3)_3$). ^{19}F NMR (282 MHz, THF-d_8): δ −76.5 (s, TFA), −79.9 (s, OTf).

[(^{t}bpy)$_2$Rh(H)(Cl)][TFA] (7). *Method 1.* [(^{t}bpy)$_2$Rh(H)(TFA)][OTf] (0.0049 g, 0.0057 mmol) was dissolved in THF-d_8 (350 μL) in a J. Young tube. CH_2Cl_2 (1.8 μL, 0.028 mmol) was added via a microsyringe. Hexamethyldisilane (HMDS, 0.2 μL) was added as an internal standard. The tube was pressurized with 25 psig of H_2(g). The reaction mixture was placed in a 70 °C oil bath for 6 days. During this time, the reaction progress was monitored by ^{1}H NMR spectroscopy until 100% conversion of [(^{t}bpy)$_2$Rh(H)(TFA)][OTf] was observed (91% yield of **7** by ^{1}H NMR spectroscopy).

Method 2. [(^{t}bpy)$_2$Rh][TFA] (0.0214 g, 0.0284 mmol) was dissolved in acetone-d_6 (1 mL) in a J. Young NMR tube. The tube was placed in the freezer (−34 °C) for 2 h. HCl (25.5 μL, 0.0255 mmol, 1 N in Et_2O) was added via a microsyringe to the tube containing the cold solution. The purple solution became a darker blackish purple upon addition of acid. After $^1/_2$ h the solvent was removed in vacuo to yield a dark black-purple solid (0.0125 g, 56%). ^{1}H NMR (300 MHz, acetone-d_6): δ 9.58 (d, $^3J_{H5-H6}$ = 6 Hz, 1H, ^{t}bpy 6), 9.26 (d, $^3J_{H5-H6}$ = 6 Hz, 1H, ^{t}bpy 6), 9.05, 8.98, 8.96, 8.90 (each a s, 1H, ^{t}bpy 3), 7.97−7.94 (m, partially buried under d at 7.94, 1H, ^{t}bpy 5), 7.94 (d, $^3J_{H5-H6}$ = 6 Hz, 2H, ^{t}bpy 5), 7.89 (d, $^3J_{H5-H6}$ = 6 Hz, 1H, ^{t}bpy 5), 7.71 (d, $^3J_{H5-H6}$ = 6 Hz, 1H, ^{t}bpy 6), 7.59 (d, $^3J_{H5-H6}$ = 6 Hz, 1H, ^{t}bpy 6), 7.50 (m, 1H, ^{t}bpy 5), 1.52 (s, 18H, ^{t}Bu), 1.38, 1.35 (each a s, 9H, ^{t}Bu), −14.37 (bs, 1H, Rh−*H*). Note: In THF-d_8 the hydride resonance is observed as a doublet with $^1J_{Rh-H}$ = 12 Hz. ^{1}H NMR (300 MHz, THF-d_8): δ −14.42 (d, $^1J_{Rh-H}$ = 12 Hz, 1H, Rh−*H*). ^{13}C NMR (201 MHz, acetone-d_6): δ 165.4, 165.0, 165.0, 164.8, 157.9, 157.4, 157.3, 154.9, 152.3, 150.8, 148.7, 126.2, 125.4, 125.0, 124.9, 122.9, 122.8, 122.7, 122.1 (each a s, ^{t}bpy aromatic C's, one signal missing presumably due to coincidental overlap), 36.6, 36.5, 36.4, 36.3 (each a s, $C(CH_3)_3$), 30.6, 30.6, 30.5, 30.4 (each a s, $C(CH_3)_3$). ^{19}F NMR (282 MHz, acetone-d_6): δ −74.9 (s, TFA).

[(^{t}bpy)$_2$Rh][TFA]. (COE)$_2$Rh(TFA) (0.0685 g, 0.152 mmol) was dissolved in THF (∼5 mL). ^{t}bpy (0.0815 g, 0.304 mmol) in THF (∼2 mL) was slowly added, causing the golden yellow solution to turn dark purple. After the mixture was stirred for 30 min, the solvent was removed under vacuum. The dark purple solid was further dried under vacuum for approximately 3 h. The solid was transferred to a fine-porosity frit and washed with benzene (5 × 2 mL) to remove free ^{t}bpy. The dark purple solid was dried under vacuum overnight (0.0908 g, 79%). ^{1}H NMR (300 MHz, acetone-d_6): δ 9.22 (d, $^3J_{H5-H6}$ = 6 Hz, 4H, ^{t}bpy 6/6′), 8.46 (s, 4H, ^{t}bpy 3/3′), 7.77 (dd, $^3J_{H5-H6}$ = 6 Hz, $^4J_{H3-H5}$ = 2 Hz, 4H, ^{t}bpy 5/5′), 1.46 (s, 36H, ^{t}Bu). ^{13}C NMR (201 MHz, acetone-d_6): δ 160.7, 156.0, 151.3, 123.9, 119.8 (each a s, ^{t}bpy aromatic C's), 35.4 (s, $C(CH_3)_3$), 29.5 (s, $C(CH_3)_3$). ^{19}F NMR (282 MHz, acetone-d_6): δ −75.0 (s, TFA). MS ($M^+ = C_{36}H_{48}N_4Rh^+$; *m*/*z* obsd, *m*/*z* calcd, ppm): 639.2899, 639.2929, −4.7.

[(^{t}bpy)$_2$Rh(Cl)$_2$][TFA] (8). *Method 1.* [(^{t}bpy)$_2$RhCl$_2$]Cl (0.2536 g, 0.3399 mmol) was dissolved in 1,2-dichlorobenzene (12 mL). HTFA (155 μL, 2.02 mmol) was added via a microsyringe. The yellow solution was heated at reflux overnight. After the solution was cooled to room temperature, Et_2O (∼25 mL) was added via the condenser. The reaction mixture was placed in the freezer (−34 °C) for several hours to allow for maximum precipitation. The reaction mixture was filtered through a fine-porosity frit, and the solid was washed with Et_2O and was dried under vacuum for approximately 1 h. The solid was reconstituted in CH_2Cl_2 (∼30 mL) and washed with H_2O (3 × 75 mL). The combined organic extracts were washed with $NaHCO_3$ (1 × 75 mL), dried over Na_2SO_4, and then reduced to dryness using a rotary evaporator. The yellow solid was dried under vacuum overnight. The solid was reconstituted in CH_2Cl_2 and precipitated with Et_2O. The solid was collected by filtering through a fine-porosity frit, washed with Et_2O, and dried under vacuum (0.207 g, 75%).

Method 2. [(^{t}bpy)$_2$Rh(OMe)$_2$][TFA] (0.296 g, 0.0363 mmol) was suspended in THF (∼8 mL). HTFA stock solution in THF (56 μL, 0.65 M) was added via a microsyringe. The reaction mixture was

dx.doi.org/10.1021/ic500636m | *Inorg. Chem.* 2014, 53, 5328−5340

stirred to dissolve the complex. The yellow solution was transferred to a glass Fisher-Porter reaction vessel. The vessel was sealed and removed from the glovebox. The Fisher-Porter vessel was pressurized with 40 psig of H_2(g) and placed in a 70 °C oil bath for 16.5 h. The solution was dark brown upon removal from the oil bath. After it was cooled to room temperature, the solution was degassed and brought into the glovebox. The solvent was removed under vacuum. The hydride product mixture was dissolved in CH_2Cl_2. The vessel was sealed and removed from the glovebox. The vessel was pressurized with 25 psig of H_2(g) and placed in a 70 °C oil bath to heat for 23.5 h. After it was cooled to room temperature, the solution was degassed and brought into the glovebox. The yellow solution was reduced to dryness under vacuum. The residue was reconstituted in DCM, and Et_2O was added to precipitate a pale yellow solid, which was collected by filtration through a fine-porosity frit, washed with Et_2O, and dried under vacuum (0.0125 g, 42%). ^{1}H NMR (800 MHz, CD_3CN): δ 9.66 (d, $^3J_{H5-H6}$ = 6 Hz, 2H, ^{t}bpy 6/6′), 8.58 (d, $^4J_{H3-H5}$ = 2 Hz, 2H, ^{t}bpy 3/3′), 8.46 (d, $^4J_{H3-H5}$ = 2 Hz, 2H, ^{t}bpy 3/3′), 8.01 (dd, $^3J_{H5-H6}$ = 6 Hz, $^4J_{H3-H5}$ = 2 Hz, 2H, ^{t}bpy 5/5′), 7.51 (d, $^3J_{H5-H6}$ = 6 Hz, 2H, ^{t}bpy 6/6′), 7.43 (dd, $^3J_{H5-H6}$ = 6 Hz, 2 Hz, 2H, ^{t}bpy 5/5′), 1.56 (s, 18H, ^{t}Bu), 1.37 (s, 18H, ^{t}Bu). ^{13}C NMR (201 MHz, CD_3CN): δ 167.3, 166.9, 156.9, 156.8, 152.3, 150.8, 126.9, 126.3, 123.5, 123.5 (each a s, ^{t}bpy aromatic C's), 36.9, 36.6 (each a s, $C(CH_3)_3$), 30.5, 30.3 (each a s, $C(CH_3)_3$). ^{19}F NMR (282 MHz, CD_3CN): δ −75.6 (s, TFA). Anal. Calcd for $C_{38}H_{48}Cl_2F_3N_4O_2Rh$: C, 55.41; H, 5.87; N, 6.80. Found: C, 55.13; H, 5.85; N, 6.93. MS ($M^+ = C_{36}H_{48}Cl_2N_4Rh^+$; *m/z* obsd, *m/z* calcd, ppm): 709.2306, 709.2318, −1.7.

[(^{t}bpy)$_2$Rh(Br)$_2$][TFA] (9). *Method 1.* [(^{t}bpy)$_2$Rh(Br)$_2$]Br (0.0253 g, 0.0288 mmol) was suspended in CH_3CN (∼5 mL). NaTFA (0.0040 g, 0.029 mmol) in CH_3CN (∼2 mL) was added dropwise. The Rh starting material dissolved upon addition of the NaTFA solution; however, the solution was slightly turbid because of the NaCl precipitate. The solution was stirred at room temperature for 1 h before it was reduced to dryness under vacuum. The pale yellow solid was reconstituted in CH_3CN and the solution filtered through Celite to remove NaCl. The Celite was washed with CH_3CN. The filtrate was reduced to 1 mL in vacuo. Et_2O was added to precipitate a yellow solid that was collected by filtration through a fine-porosity frit, washed with pentane, and dried under vacuum (0.0231 g, 88%).

Method 2. [(^{t}bpy)$_2$Rh(OMe)$_2$][TFA] (0.0509 g, 0.0625 mmol) was suspended in THF (∼15 mL). HTFA (4.8 μL, 0.063 mmol) was added via a microsyringe. The reaction mixture was stirred to dissolve the complex. The yellow solution was transferred to a Fisher-Porter reaction vessel. The vessel was sealed and removed from the glovebox. The Fisher-Porter reactor was pressurized with 35 psig of H_2(g) and placed in a 70 °C oil bath for 6 h and 15 min. The solution was dark brown upon removal from the oil bath. After the solution was cooled to room temperature, the Fisher-Porter vessel was degassed and brought into the glovebox. CH_2Br_2 (86 μL, 1.2 mmol) was added via a microsyringe. The vessel was sealed and removed from the glovebox. The vessel was pressurized with 20 psig of H_2(g) and placed in a 70 °C oil bath to heat for 6.5 h. The THF-insoluble yellow solid was collected by filtration and washed with hexanes and pentane. The filtrate was reduced to 1 mL in vacuo. Hexanes was added to the filtrate to precipitate a yellow solid, which was collected in the same frit as the initial solid. The solid was washed with hexanes and dried under vacuum (0.0392 g, 69%). ^{1}H NMR (800 MHz, CD_3CN): δ 9.98 (d, $^3J_{H5-H6}$ = 6 Hz, 2H, ^{t}bpy 6/6′), 8.71 (s, 2H, ^{t}bpy 3/3′), 8.59 (s, 2H, ^{t}bpy 3/3′), 8.09 (dd, $^3J_{H5-H6}$ = 6 Hz, $^4J_{H3-H5}$ = 2 Hz, 2H, ^{t}bpy 5/5′), 7.59 (d, $^3J_{H5-H6}$ = 6 Hz, 2H, ^{t}bpy 6/6′), 7.56 (dd, $^3J_{H5-H6}$ = 6 Hz, $^4J_{H3-H5}$ = 2 Hz, 2H, ^{t}bpy 5/5′), 1.67 (s, 18H, ^{t}Bu), 1.48 (s, 18H, ^{t}Bu). ^{13}C NMR (201 MHz, CD_3CN): δ 167.1, 166.9, 156.9, 156.8, 154.2, 150.4, 127.2, 126.3, 123.7, 123.6 (each a s, ^{t}bpy aromatic C's), 36.9, 36.6 (each a s, $C(CH_3)_3$), 30.5, 30.3 (each a s, $C(CH_3)_3$. ^{19}F NMR (282 MHz, acetone-d_6): δ −75.4 (s, TFA). MS ($M^+ = C_{36}H_{48}Br_2N_4Rh^+$; *m/z* obsd, *m/z* calcd, ppm): 797.1330 (46.5), 797.1295 (49.4), 4.4; 798.1340 (19.4), 798.1327 (20.2), 1.6; 799.1306 (100), 799.1278 (100), 3.5; 800.1320 (40.3), 800.1308 (39.9), 1.5; 801.1284 (56.6), 801.1267 (54.6), 2.1; 802.1305 (20.2), 802.1290 (20.2), 1.9.

[(^{t}bpy)$_2$Rh(MeOH)$_2$][OTf][TFA]$_2$ (3). This complex is obtained as an insoluble byproduct from the protonation of [(^{t}bpy)$_2$Rh(OMe)$_2$][OTf] with 1 equiv of HTFA. Complex **3** has been independently synthesized as follows. [(^{t}bpy)$_2$Rh(OMe)$_2$][OTf] (0.0385 g, 0.0452 mmol) was suspended in THF (∼5 mL). HTFA (7 μL, 0.091 mmol) was added slowly. The addition of HTFA resulted in dissolution of [(^{t}bpy)$_2$Rh(OMe)$_2$][OTf]. After the mixture was stirred for 4 h, the solvent was removed in vacuo. The yellow solid was redissolved in CH_2Cl_2 and precipitated with pentane. The pale yellow solid was collected via filtration though a fine porosity frit, washed with pentane (2 × 2.5 mL), and dried under vacuum (0.0267 g, 55%). ^{1}H NMR (300 MHz, CD_2Cl_2): δ 9.42 (d, $^3J_{H5-H6}$ = 6 Hz, 2H, 6/6′), 8.41 (s, 2H, ^{t}bpy 3/3′), 8.27 (s, 2H, ^{t}bpy 3/3′), 7.99 (d, $^3J_{H5-H6}$ = 6 Hz, 2H, 6/6′), 7.43 (s, 4H, ^{t}bpy 5/5′), 2.84 (s, 6H, CH_3OH), 1.58 (s, 18H, ^{t}Bu), 1.36 (s, 18H, ^{t}Bu). ^{13}C NMR (151 MHz, CD_2Cl_2): δ 167.7, 166.4, 156.7, 156.1, 151.5, 150.0, 126.3, 126.1, 122.2, 122.0 (each a s, ^{t}bpy aromatic C's), 36.7, 36.3 (each a s, $C(CH_3)_3$), 30.8, 30.4 (each a s, $C(CH_3)_3$). A HSQC experiment confirms that the CH_3OH resonance is missing due to coincidental overlap with the solvent resonance. ^{13}C NMR (201 MHz, acetone-d_6): δ 167.6, 166.4, 157.0, 157.0, 152.0, 150.2, 126.3, 126.2, 123.3, 123.1 (each a s, ^{t}bpy aromatic C's), 53.1 (s, CH_3OH), 36.9, 36.4 (each a s, $C(CH_3)_3$), 30.6, 30.2 (each a s, $C(CH_3)_3$). ^{19}F NMR (282 MHz, CD_2Cl_2): δ −77.0 (s, TFA), −80.0 (s, OTf). Anal. Calcd for $C_{43}H_{56}F_9N_4O_9RhS$: C, 47.87; H, 5.23; N, 5.19. Found: C, 47.81; H, 5.27; N, 5.33.

H_2 Activation: Kinetic Studies. A representative catalytic reaction is described. [(^{t}bpy)$_2$Rh(OMe)$_2$][OTf] (0.0360 g, 0.0423 mmol) was suspended in THF-d_8 (2 mL) in a volumetric flask. The mixture was stirred to dissolve as much solid as possible. HTFA (3.2 μL, 0.042 mmol) was added slowly dropwise. The solution was stirred, causing all of the [(^{t}bpy)$_2$Rh(OMe)$_2$][OTf] to dissolve. HMDS (1 μL, 0.0049 mmol) was added as an internal standard. The homogeneous yellow solution was transferred to a tube. A stir bar was added, the tube was capped, and the solution was stirred (300 rpm) for 12 h. Within 15 min, a yellow solid precipitated. After 12 h, the tube was removed from the glovebox and centrifuged for 5 min. The tube was taken into a glovebox, where the yellow solution was decanted from the yellow solid. The solution (300 μL each) was added to five J. Young tubes. For some experiments, MeOH was added at this point. Either 3 equiv of methanol (0.8 μL, 0.02 mmol) or 5 equiv of methanol (1.3 μL, 0.032 mmol) was added to each tube. The amount of methanol was based on the moles of [(^{t}bpy)$_2$Rh(OMe)$_2$][OTf] added to the volumetric flask and how much of this stock solution was added to each tube (0.0063 mmol/tube). The tubes were all frozen with N_2(l). Before insertion into the NMR probe, each tube was degassed using three freeze−pump−thaw cycles. The tubes were left under vacuum for 30 s during these cycles. The tubes were then pressurized with H_2 (15, 30, 45, or 55 psig) or D_2 for 15 s and inverted several times to ensure adequate mixing. The tubes were placed into a temperature-calibrated Varian 500 MHz spectrometer probe (equilibrated at 68 °C). The temperature was determined using 80% ethylene glycol in DMSO-d_6 and the following equation provided by Bruker Instruments, Inc. VT-Calibration Manual: T (K) = (4.218 − Δ)/0.009132, where Δ is the shift difference (ppm) between CH_2 and OH resonances of ethylene glycol. ^{1}H NMR arrays were collected. Eight scans were acquired for each spectrum. The delay time was set to 12.8 s, and the acquisition time was set to 2.2 s. Each spectrum required 2 min to complete. Depending on the experiment, collection of a new data point began every 120 or 180 s. Each set of conditions was run at least in triplicate, except for experiments with 20 psig and 30 psig of D_2, which were only performed once.

[(^{t}bpy)$_2$Rh(OMe)(MeOH)][OTf][TFA] (4). Complex **4** was generated in situ during the experimental setup for H_2 activation (see above). X-ray-quality crystals were grown in the crystal tube containing [(^{t}bpy)$_2$Rh(MeOH)$_2$][OTf][TFA]$_2$, from which the stock solution was decanted, and any residual solution remaining in the crystal tube after decanting (hence, there is some [(^{t}bpy)$_2$Rh(OMe)(MeOH)][OTf][TFA] present). DCM was added to the crystal tube, and the

dx.doi.org/10.1021/ic500636m | *Inorg. Chem.* 2014, 53, 5328−5340

solution was layered with pentane. ^{1}H NMR (300 MHz, THF-d_8): δ 9.43 (d, $^3J_{H5-H6}$ = 6 Hz, 2H, ^{t}bpy 6/6′), 8.83 (d, $^4J_{H3-H5}$ = 2 Hz, 2H, ^{t}bpy 3/3′), 8.65 (d, $^4J_{H3-H5}$ = 2 Hz, 2H, ^{t}bpy 3/3′), 8.07 (dd, $^3J_{H5-H6}$ = 6, $^4J_{H3-H5}$ = 2 Hz, 2H, ^{t}bpy 5/5′), 7.56 (d, $^3J_{H5-H6}$ = 6 Hz, 2H, ^{t}bpy 6/6′), 7.49 (dd, $^3J_{H5-H6}$ = 6 Hz, $^4J_{H3-H5}$ = 2 Hz, 2H), 2.84 (s, 6H, OCH_3/CH_3OH), 1.58, 1.34 (each a s, 18H, ^{t}bpy). ^{13}C NMR (201 MHz, THF-d_8): δ 167.4, 165.8, 157.5, 157.0, 152.3, 150.1, 126.4, 125.9, 123.3, 123.1 (each a s, ^{t}bpy), 54.85 (s, OCH_3), 36.90, 36.43 (each a s, $C(CH_3)_3$), 30.60, 30.33 (each a s, $C(CH_3)_3$). ^{19}F NMR (282 MHz, THF-d_8): δ −76.8 (s, TFA), −80.1 (OTf). Anal. Calcd for $C_{41}H_{55}F_6N_4O_7RhS$ C, 51.04; H, 5.75; N, 5.81. Found: C, 50.46; H, 5.61; N, 5.71. [(^{t}bpy)$_2$Rh(OMe)(TFA)][OTf] (**5**) is obtained as the minor soluble product from the reaction of [(^{t}bpy)$_2$Rh(OMe)$_2$][OTf] (**1**) with HTFA (1 equiv). Complex **5** has not been isolated. ^{1}H NMR for [(^{t}bpy)$_2$Rh(OMe)(TFA)][OTf] (**5**) (500 MHz, THF-d_8): δ 9.48 (d, $^3J_{H5-H6}$ = 6 Hz, 1H, ^{t}bpy 6), 9.33 (d, $^3J_{H5-H6}$ = 6 Hz, 1H, ^{t}bpy 6), 9.08 (d, $^3J_{H5-H6}$ = 6 Hz, 1H, ^{t}bpy 6), 8.76 (s, 1H, ^{t}bpy 3), 8.71 (s, 1H, ^{t}bpy 3), 8.52 (s, 2H, ^{t}bpy 3), 8.14 (dd, $^3J_{H5-H6}$ = 6 Hz, $^4J_{H3-H5}$ = 2 Hz, 1H, ^{t}bpy 5), 7.76 (d, J = 6 Hz, 1H, ^{t}bpy 6), 7.59 (unresolved dd, 1H, ^{t}bpy 5), 7.43 (dd, $^3J_{H5-H6}$ = 6 Hz, $^4J_{H3-H5}$ = 2 Hz, 1H, ^{t}bpy 5), 7.36 (d, $^3J_{H5-H6}$ = 6 Hz, 1H, ^{t}bpy 5), 1.44 (s, 9H, ^{t}Bu), 1.38 (s, 9H, ^{t}Bu). The remaining two ^{t}Bu resonances and OMe resonance are missing presumably due to coincidental overlap with resonances for [(^{t}bpy)$_2$Rh(OMe)(MeOH)][OTf][TFA] (**4**).

Methanol Exchange. The general procedure described above for the H_2 activation kinetic studies was utilized with the following modifications. After the solution (300 μL each) was added to five J. Young tubes, 5 equiv (1.3 μL, 0.032 mmol), 10 equiv (2.6 μL, 0.064 mmol), or 20 equiv of CD_3OD (5.3 μL, 0.13 mmol) relative to [(^{t}bpy)$_2$Rh(OMe)$_2$][OTf] was added to each tube. Room-temperature ^{1}H NMR spectra were acquired. The tubes were placed into a temperature-calibrated Varian 500 MHz spectrometer probe (equilibrated at 68 °C). The temperature was determined as described above. ^{1}H NMR arrays were collected. Eight scans were acquired for each spectrum. The delay time was set to 12.8 s, and the acquisition time was set to 2.2 s. Each spectrum required 2 min to complete. Acquisition of a new data point began every 180 s. The procedure was repeated using 5 and 10 equiv of CD_3OD.

Methanol Exchange: Coordinated CD_3OD with CH_3OH. The general procedure described above for the H_2 activation kinetic studies was utilized with the following modifications. [(^{t}bpy)$_2$Rh(OCD_3)$_2$][OTf] was prepared using the procedure for the synthesis of complex **1**, except CD_3OD was used instead of protio methanol. The ^{1}H NMR data for [(^{t}bpy)$_2$Rh(OCD_3)$_2$][OTf] are identical with those of perprotio complex **1**, except the methoxide peak is absent. The deuterated complex [(^{t}bpy)$_2$Rh(OCD_3)$_2$][OTf] was treated with 1 equiv of DTFA. The solution (300 μL each) was divided equally into five J. Young NMR tubes, and 5 equiv (1.3 μL, 0.032 mmol) of MeOH was added to each tube. Room-temperature ^{1}H NMR spectra were acquired. The tubes were placed into a temperature-calibrated Varian 500 MHz spectrometer probe (equilibrated at 68 °C). The temperature was determined as described above. ^{1}H NMR arrays were collected. Eight scans were acquired for each spectrum. The delay time was set to 12.8 s, and the acquisition time was set to 2.2 s. Acquisition of a new data point began every 180 s. The appearance for the coordinated MeOH resonance was monitored and analyzed using first-order fits.

Hg Poisoning Test. The general procedure described above for the H_2 activation kinetic studies was utilized with the following modifications. After the solution (300 μL each) was added to five J. Young tubes, a drop of Hg was added to each tube. Before insertion into the NMR probe, the tube was degassed using three freeze−pump−thaw cycles. The tube was left under vacuum for 30 s during these cycles. The tube was pressurized with H_2 (45 pisg) for 15 s and inverted several times to ensure adequate mixing. The tube was placed into a temperature-calibrated Varian 500 MHz spectrometer probe (equilibrated at 68 °C). The temperature was determined as described above. A ^{1}H NMR array was collected. Eight scans were acquired for each spectrum. The delay time was set to 12.8 s, and the acquisition time was set to 2.2 s. Each spectrum required 2 min to complete. Acquisition of a new data point began every 180 s.

■ ASSOCIATED CONTENT

Ⓢ Supporting Information

Figures, tables, and CIF files giving ^{1}H and ^{13}C NMR spectra for complexes **6** and **7**, computational details, and crystallographic data for complexes **2** and **4**. This material is available free of charge via the Internet at http://pubs.acs.org.

■ AUTHOR INFORMATION

Corresponding Authors

*E-mail for D.H.E.: dhe@chem.byu.edu.

*E-mail for T.B.G.: tbg7h@virginia.edu.

Notes

The authors declare no competing financial interest.

■ ACKNOWLEDGMENTS

T.B.G. acknowledges support from the U.S. National Science Foundation under award number CHE-1152812. T.B. acknowledges support via a postdoctoral fellowship from the MICINN of Spain. The authors acknowledge support of the National Science Foundation (CHE-1126602) for the purchase of an X-ray diffractometer at the University of Virginia. D.H.E. thanks BYU and the Fulton Supercomputing Lab. The authors thank Jeffery Dahl at Shimadzu Scientific Instruments, Columbia, MD, and Joe Hedrick of Agilent Technologies, Wilmington, DE, for collection of HRMS data and Professor Mahdi Abu-Omar (Purdue University) for useful discussions.

■ REFERENCES

(1) Hartwig, J. F. *Organotransition Metal Chemistry: From Bonding to Catalysis*; University Science Books: Sausalito, CA, 2010.

(2) Crabtree, R. H. *The Organometallic Chemistry of the Transition Metals*, 4th ed.; Wiley: New York, 2005.

(3) *Handbook of Homogeneous Hydrogenation*; Wiley-VCH: Weinheim, Germany, 2007.

(4) Clapham, S. E.; Hadzovic, A.; Morris, R. H. *Coord. Chem. Rev.* **2004**, *248*, 2201.

(5) Deutsch, C.; Krause, N.; Lipshutz, B. H. *Chem. Rev.* **2008**, *108*, 2916.

(6) Sergeev, A. G.; Hartwig, J. F. *Science* **2011**, *332*, 439.

(7) Furimsky, E. *Appl. Catal., A* **2000**, *199*, 147.

(8) Fryzuk, M. D.; Montgomery, C. D.; Rettig, S. J. *Organometallics* **1991**, *10*, 467.

(9) Tenn, W. J., III; Young, K. J. H.; Oxgaard, J.; Nielson, R. J.; Goddard, W. A., III; Periana, R. A. *Organometallics* **2006**, *25*, 5173.

(10) Fulmer, G. R.; Muller, R. P.; Kemp, R. A.; Goldberg, K. I. *J. Am. Chem. Soc.* **2009**, *131*, 1346.

(11) Fulmer, G. R.; Herndon, A. N.; Kaminsky, W.; Kemp, R. A.; Goldberg, K. I. *J. Am. Chem. Soc.* **2011**, *133*, 17713.

(12) Kloek, S. M.; Heinekey, D. M.; Goldberg, K. I. *Angew. Chem., Int. Ed.* **2007**, *46*, 4736.

(13) Hanson, S. K.; Heinekey, D. M.; Goldberg, K. I. *Organometallics* **2008**, *27*, 1454.

(14) Bercaw, J. E.; Hazari, N.; Labinger, J. A. *Organometallics* **2009**, *28*, 5489.

(15) Ahmed, T. S.; Tonics, I. A.; Labinger, J. A.; Bercaw, J. E. *Organometallics* **2013**, *32*, 3322.

(16) Webb, J. R.; Pierpont, A. W.; Munro-Leighton, C.; Gunnoe, T. B.; Cundari, T. R.; Boyle, P. D. *J. Am. Chem. Soc.* **2010**, *132*, 4520.

(17) Lohr, T. L.; Piers, W. E.; Parvez, M. *Chem. Sci.* **2013**, *4*, 770.

(18) Sakamoto, M.; Ohki, Y.; Kehr, G.; Erker, G.; Tatsumi, K. *J. Organomet. Chem.* **2009**, *694*, 2820.

(19) Seino, H.; Misumi, Y.; Hojo, Y.; Mizobe, Y. *Dalton Trans.* **2010**, *39*, 3072.

(20) Misumi, Y.; Seino, H.; Mizobe, Y. *J. Am. Chem. Soc.* **2009**, *131*, 14636.
(21) Widegren, J. A.; Finke, R. G. *J. Mol. Catal. A: Chem.* **2003**, *198*, 317.
(22) Frisch, M. J.; Trucks, G. W.; Schlegel, H. B.; Scuseria, G. E.; Robb, M. A.; Cheeseman, J. R.; Scalmani, G.; Barone, V.; Mennucci, B.; Petersson, G. A.; Nakatsuji, H.; Caricato, M.; Li, X.; Hratchian, H. P.; Izmaylov, A. F.; Bloino, J.; Zheng, G.; Sonnenberg, J. L.; Hada, M.; Ehara, M.; Toyota, K.; Fukuda, R.; Hasegawa, J.; Ishida, M.; Nakajima, T.; Honda, Y.; Kitao, O.; Nakai, H.; Vreven, T.; Montgomery, J. A., Jr.; Peralta, P. E.; Ogliaro, F.; Bearpark, M.; Heyd, J. J.; Brothers, E.; Kudin, K. N.; Staroverov, V. N.; Kobayashi, R.; Normand, J.; Raghavachari, K.; Rendell, A.; Burant, J. C.; Iyengar, S. S.; Tomasi, J.; Cossi, M.; Rega, N.; Millam, N. J.; Klene, M.; Knox, J. E.; Cross, J. B.; Bakken, V.; Adamo, C.; Jaramillo, J.; Gomperts, R.; Stratmann, R. E.; Yazyev, O.; Austin, A. J.; Cammi, R.; Pomelli, C.; Ochterski, J. W.; Martin, R. L.; Morokuma, K.; Zakrzewski, V. G.; Voth, G. A.; Salvador, P.; Dannenberg, J. J.; Dapprich, S.; Daniels, A. D.; Farkas, Ö.; Foresman, J. B.; Ortiz, J. V.; Cioslowski, J.; Fox, D. J. *Gaussian 09*, revision B.01 ; Gaussian, Inc.: Wallingford, CT, 2009.
(23) Zhao, Y.; Truhlar, D. G. *Theor. Chem. Acc.* **2008**, *120*, 215.
(24) Zhao, Y.; Truhlar, D. G. *Acc. Chem. Res.* **2008**, *41*, 157.
(25) Marenich, A. V.; Cramer, C. J.; Truhlar, D. G. *J. Phys. Chem. B* **2009**, *113*, 6378.
(26) Kubas, G. J. *Metal Dihydrogen and σ-Bond Complexes*; Kluwer Academic/Plenum Publishers: New York, 2001; p 259.
(27) Jessop, P. G.; Morris, R. H. *Coord. Chem. Rev.* **1992**, *121*, 155.
(28) Conner, D.; Jayaprakash, K. N.; Cundari, T. R.; Gunnoe, T. B. *Organometallics* **2004**, *23*, 2724.
(29) Ess, D. H.; Bischof, S. M.; Oxgaard, J.; Periana, R. A.; Goddard, W. A. *Organometallics* **2008**, *27*, 6440.
(30) Webb, J. R.; Munro-Leighton, C.; Pierpont, A. W.; Gurkin, J. T.; Gunnoe, T. B.; Cundari, T. R.; Sabat, M.; Petersen, J. L.; Boyle, P. D. *Inorg. Chem.* **2011**, *50*, 4195.
(31) Jimenez-Tenorio, M.; Puerta, M. C.; Valerga, P.; Ortuno, M. A.; Ujaque, G.; Lledos, A. *Inorg. Chem.* **2013**, *52*, 8919.
(32) Morris, R. H. *J. Am. Chem. Soc.* **2014**, *136*, 1948.
(33) Yakelis, N. A.; Bergman, R. G. *Organometallics* **2005**, *24*, 3579.
(34) Bolinger, C. M.; Story, N.; Sullivan, B. P.; Meyer, T. J. *Inorg. Chem.* **1988**, *27*, 4582.
(35) Schrock, R. R.; Osborn, J. A. *J. Am. Chem. Soc.* **1971**, *93*, 3089.
(36) Yan, S. G.; Brunschwig, B. S.; Creutz, C.; Fujita, E.; Sutin, N. *J. Am. Chem. Soc.* **1998**, *120*, 10553.